Progress in the preparation and evaluation of glucose-sensitive microneedle systems and their blood glucose regulation

Yu Wang,[a] Haojie Yu, ID *[a,b] Li Wang, ID [a,b] Jian Hu[c] and Jingyi Feng[c]

Glucose-sensitive microneedle systems (GSMSs) as an intelligent strategy for treating diabetes can well solve the problems of puncture pain, hypoglycemia, skin damage, and complications caused by the subcutaneous injection of insulin. According to the various functions of each component, herein, therapeutic GSMSs are reviewed based on three parts (glucose-sensitive models, diabetes medications, and microneedle body). Moreover, the characteristics, benefits, and drawbacks of three types of typical glucose-sensitive models (phenylboronic acid based polymer, glucose oxidase, and concanavalin A) and their drug delivery models are reviewed. In particular, phenylboronic acid-based GSMSs can provide a long-acting drug dose and controlled release rate for the treatment of diabetes. Moreover, their painless, minimally invasive puncture also greatly improves patient compliance, treatment safety, and potential application prospects.

1. Introduction

Presently, diabetes is one of the most prevalent and widespread diseases, affecting a large portion of the global population.[1] Simultaneously, diabetes is also accompanied by numerous cardiovascular and cerebrovascular complications,[2] such as hypertension[3] and hyperlipidemia,[4] which pose a significant threat to human health. Therefore, research on the treatment of diabetes is ongoing, ranging from the development of various hypoglycemic drugs to the evolution of various treatment methods, aiming to improve the two major causes of the disease, impaired insulin secretion and insulin resistance, to develop therapeutic systems that can replace the damaged pancreas in diabetic patients to the greatest extent and improve the internal environment of patients. Accordingly, huge financial expenditures and scientific research efforts have been invested to achieve these goals.[5–7]

The traditional treatments for type 1 diabetes and type 2 diabetes are insulin injections and oral hypoglycemic drugs.[8,9] However, these two treatment methods are associated with certain problems such as low drug utilization rate and uncontrollable drug effect.[10,11] When the drug cannot work adequately, it may lead to an insufficient reduction in the blood glucose, and thus a better therapeutic effect cannot be achieved. Conversely, when the drug works too quickly or in excess, it will lead to hypoglycemia,[12] with dangerous side effects. Frequent insulin injection therapy is associated with obvious physical pain to patients and causes them to have strong psychological resistance.[13] In addition, it is not suitable for the long-term stable treatment of diabetes,[14] and thus an extremely mild pain and drug release controllable therapeutic system is a better choice.

Therapeutic glucose-sensitive microneedle systems (GSMSs) are usually composed of three parts, including a polymer-based microneedle body, glucose-sensitive model, and hypoglycemic drug. The micron-scale microneedle body can pierce the skin, deliver the glucose-sensitive model and hypoglycemic drug to the dermis,[15] and then use the glucose-sensitive model to identify the free distributed glucose in the tissue fluid and release the hypoglycemic drug in the corresponding concentration according to the difference in glucose concentration. As a new type of treatment, GSMSs can significantly reduce the pain and skin wounds of injection treatment,[16] and greatly improve the controllability of drug utilization and drug release.[17] They provide diabetic patients with a portable transdermal drug delivery method that can adapt to differences in blood glucose concentrations of individuals[18,19] and improves patient compliance with more efficient and safe treatment.

Herein, we discuss the establishment and differences between three types of glucose-sensitive models in therapeutic GSMSs, as well as their glucose-sensitive mechanism and drug release. In particular, the preparation and classification of

[a]State Key Laboratory of Chemical Engineering, College of Chemical and Biological Engineering, Zhejiang University, Hangzhou 310058, P. R. China. E-mail: hjyu@zju.edu.cn
[b]Zhejiang-Russia Joint Laboratory of Photo-Electro-Magnetic Functional Materials, College of Chemical and Biological Engineering, Zhejiang University, Hangzhou 310058, P. R. China
[c]Key Laboratory of Clinical Evaluation Technology for Medical Device of Zhejiang Province, The First Affiliated Hospital, College of Medicine, Zhejiang University, Hangzhou 310003, P.R. China

glucose response models are innovatively summarized. This provides a very instructive view on the drug delivery requirements in different application scenarios. The way the drugs are loaded and their interactions with the drugs in the glucose response model are also described in detail. This presents good suggestions for the existing inexplicable phenomena and laws of drug loading and controlled release. Furthermore, the advantages and existing problems associated with the use of phenylboronic acid groups as glucose-sensitive models are summarized. In the case of GSMSs based on phenylboronic acid, a more efficient design idea and preparation process screening are demonstrated. Regarding the practical application background of GSMS, this review proposes more realistic requirements. Finally, the mechanical properties and therapeutic effects of GSMS are analyzed and evaluated. Through the targeted analysis of the selection of each component material and the interaction between the components in therapeutic GSMSs, an optimized scheme is proposed, which is helpful to establish GSMSs with practical application value and convenient large-scale production. Meanwhile, this review also presents the first summary of GSMS systems in terms of the blood glucose control effect and the standards that need to be achieved before clinical application. From the preparation of GSMSs to their therapeutic application and safety assessment, a comprehensive evaluation system and strong guidelines are provided.

2. Construction and advantages of GSMS

According to the latest statistics in the 10th edition of the International Diabetes Federation (IDF) Diabetes Research Atlas. The global total population reached 7.9 billion in 2021, and the proportion of diabetic patients was as high as 536.6 million, with 6.7 million patients dying of diabetes and its complications.[1] However, there are still numerous issues associated with monitoring blood glucose in pre-diabetic patients and the control of blood glucose during this disease. The goal of diabetes therapeutic systems is to create more intelligent diabetes monitoring and treatment techniques. Meanwhile, the aim is also to reduce patient suffering and enhance the effectiveness of diabetes treatments.[20,21] Consequently, because of their advantages of being painless, minimally invasive, and glucose sensitive, and GSMSs have gradually shown potential to replace injection therapy.

2.1. Composition of GSMSs: microneedle body, diabetes medication, and glucose-sensitive model

Therapeutic GSMSs reduce the injection injury and improve the controllability of drug release. They can be roughly divided into three parts, as depicted in Fig. 1. The microneedle body and base patch make up the outer support structure shell, which is loaded with the drug and punctures the skin to complete percutaneous drug delivery. The core component, a glucose-sensitive model, recognizes glucose-containing sub-
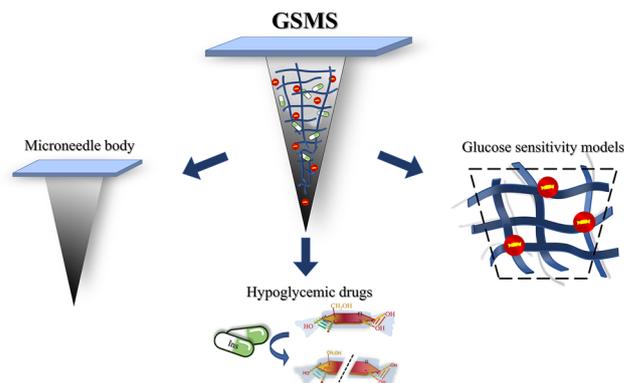

Fig. 1 Composition of glucose-sensitive microneedle system (GSMS).

stances and allows for the controlled release of medication by monitoring and reacting to the real-time blood glucose levels. The third component includes auxiliary drugs and medications that are loaded in the microneedle to lower the blood glucose levels. It can replace the damaged pancreas of patients and regulate blood glucose in a specific way.

The coordination of the different components of the microneedle system improves the efficiency of drug delivery. Each component is indispensable and plays a prominent role. Here, the glucose-sensitive model is the intelligent brain of the system. It detects the level of glucose in the environment and regulates the drug release rate and dosage according to the blood glucose level. To some extent, the components of the glucose-sensitive model can mimic how the human pancreas works. Through treatment with GSMSs, the irrelevant consumption and waste of drugs in the body can be reduced,[22] the action time of drugs can be prolonged,[23] and the utilization rate of drugs can be improved.[24]

2.2. Determination of diabetes: blood glucose standard as an example

Diabetes is a chronic condition that permanently distorts the blood glucose levels.[25] Patients with type 1 diabetes and advanced type 2 diabetes cannot complete blood glucose regulation in time and effectively due to impaired pancreatic function, resulting in a significant increase in blood glucose levels. Therefore, the glucose concentration in the blood is the most direct criterion for judging diabetes. Meanwhile, diabetes can also be diagnosed by the indicator of glycosylated hemoglobin (HbA_{1c}), and the diagnostic cut-off point is $HbA_{1c} \geq 6.5\%$.[26,27] As seen in Fig. 2, it can typically be determined that patients have a high probability of diabetes risk when their fasting blood glucose level is and exceeds 7.0 mmol L^{-1} (126 mg dL^{-1}) for a prolonged period or when their blood glucose level two hours after eating exceeds 11.1 mmol L^{-1} (200 mg dL^{-1}).[1]

2.3. Advantages of GSMSs compared with subcutaneous injection

Generally, the most effective way to treat type 1 and advanced type 2 diabetes is insulin injections.[28] Insulin is a hormone,
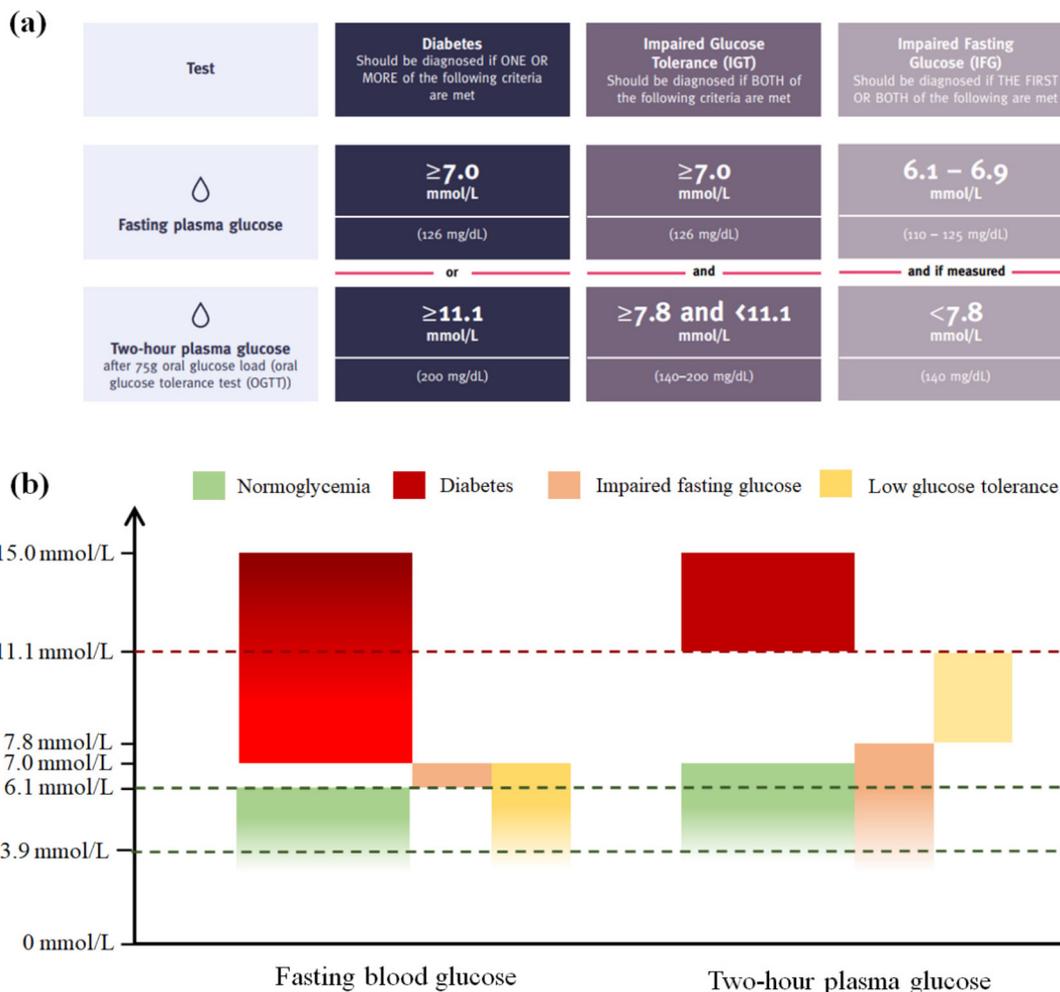
Fig. 2 (a) Modified diagnostic criteria for diabetes.[1] (b) Range of normal blood glucose, diabetic blood glucose and potential diabetes blood glucose. (The general lower limit of fasting blood glucose is 3.9 mmol L^{-1}, and 15.0 mmol L^{-1} is far beyond the range of normal blood glucose.).

and thus is not suitable for oral therapy.[29] In diabetic patients, insulin is delivered to the subcutaneous tissue through subcutaneous injection, and then through the internal circulation of the body, delivering insulin to all parts of the body. Finally, it exerts its effects on the liver, skeletal muscle, and adipose tissue.[11,30] Although the existing insulin injection therapy can achieve short-term control of the blood glucose levels, this therapy also has some drawbacks. Obviously, the injected metal needle is painful to diabetic patients.[31] In addition, the long-term injection will make the wound caused by the injection have potential lesions and the risk of infection.[32] When injecting insulin, the injection volume of the drug is poorly controllable, producing the potential risk of hypoglycemia, which can be life threatening.

Therefore, it is urgent to develop more effective and safer treatment systems. In this case, GSMSs have a micron injection needle body and a millimeter back patch, which is much smaller than the size of the syringe needle and insulin pen needle (Fig. 3).[33] The microneedle used in transdermal drug delivery only penetrates the epidermis to the dermis layer and

does not come into contact with any nerve tissues or blood vessels.[34] Accordingly, GSMSs greatly reduce the pain of puncture and skin damage. The glucose-sensitive model detects the glucose in the human tissue fluid, and then the drug is released in accordance with the glucose concentration. Therefore, GSMSs largely prevent the abrupt release of insulin and hypoglycemia caused by overdosing.[35]

3. Preparation and evaluation of glucose-sensitive models

Glucose-responsive substances can interact or specifically bind with glucose. Therefore, they are very sensitive to glucose environments with different concentrations and can be used as a glucose-sensitive model.[36] As shown in Fig. 4, the three typical glucose-sensitive models are phenylboronic-based polymer (P-PBA),[37] glucose oxidase (GOx),[38] and concanavalin A (Con A).[39] Among them, P-PBA can bind specifically with the glycols on glucose to form reversible phenylborate ester bonds.
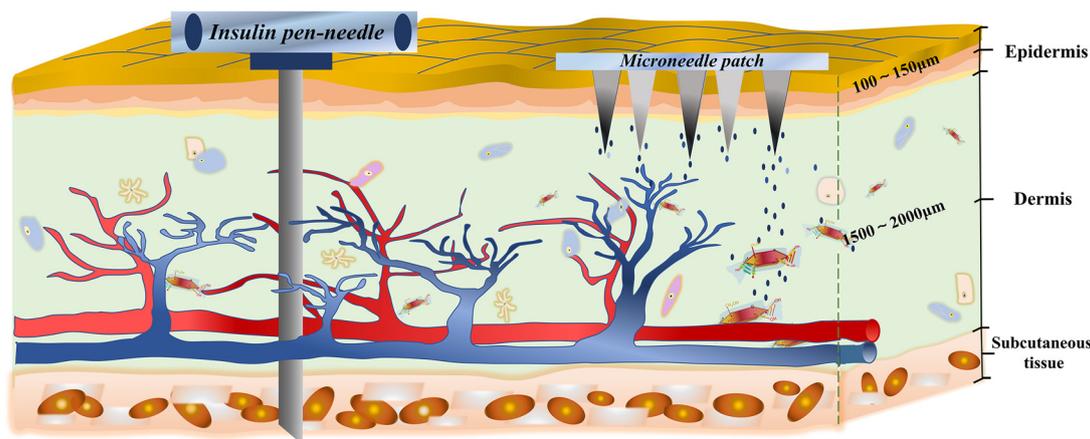
Fig. 3 Schematic diagram of microneedle system treatment on the abdominal skin.
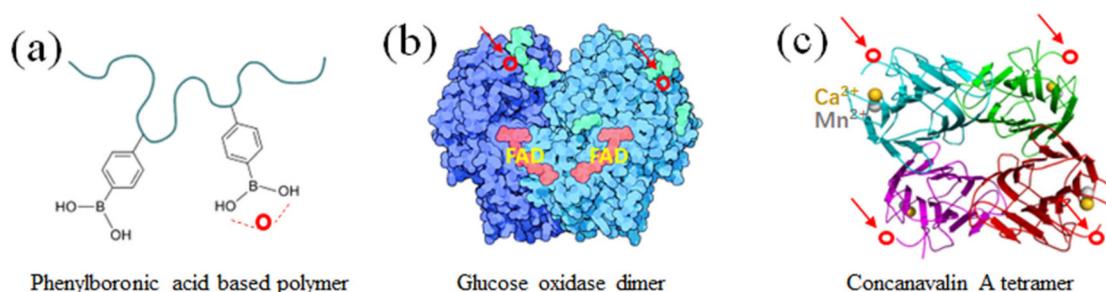

Fig. 4 Three typical glucose responsive substances. (a) Phenylboronic acid-based polymer. (b) Glucose oxidase dimer. Image from "Molecule of the Month: Glucose Oxidase" of RCSB Protein Data Bank, Goodsell D (May 2006). doi:10.2210/rcsb_pdb/mom_2006_5.[43] (c) Concanalin tetramer. Image from "Structure of concanavalin A at 2.4-A resolution" of Biochemistry, Hardman KD, Ainsworth CF (December 1972). doi:10.1021/bi00776a006 [44] (○ is the glucose-binding site).

This bond can be used as a dynamic binding point to recognize changes in glucose concentration. GOx can specifically catalyze β-D-glucose under aerobic conditions, generating gluconic acid and hydrogen peroxide. Con A is a tetramer globulin, where each of its subunits contains a sugar binding site, which can specifically bind with α-mannose and α-glucose.

However, the three different types of substances have diverse physical and chemical characteristics, such as molecular weight, solubility, stability, biological activity, biocompatibility, and biological toxicity.[40–42] These features significantly influence the structural design and manufacturing of glucose-sensitive models, further affecting their reactivity with glucose molecules. The three substance binding mechanisms for glucose and the glucose response and drug release characteristics of the three substance-based glucose sensitive models are analyzed in the subsequent sections.

3.1. Preparation of glucose-sensitive models based on phenylboronic acid (P-PBA) and their response characteristics

The dynamic hydrolysis equilibrium of the phenylboronic acid group in aqueous solution is depicted in Scheme 1.[45] Boron atoms will combine with hydroxyl ions to form a tetrahedral structure,[46] making the phenylboronic acid group change from
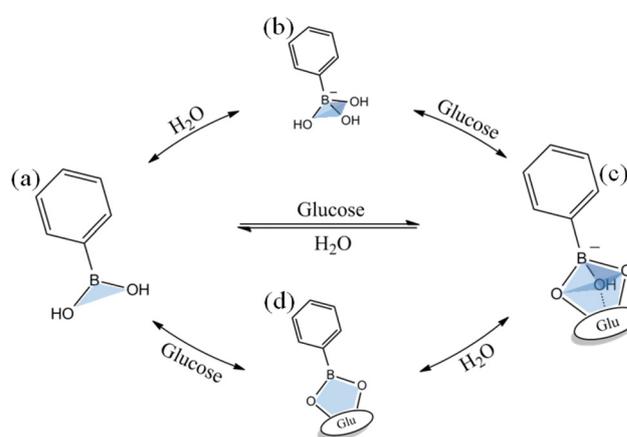
Scheme 1 Schematic diagram of the binding of phenylboronic acid groups to glucose in solution.

uncharged to negatively charged.[47] Subsequently, the phenylboronic acid group in the hydrolytic state is more likely to specifically bind with glucose molecules to form dynamic borate ester bonds.[48] Given that the phenylborate group combines with glucose to form a borate ester bond, the polyhy-

droxy structure in glucose also significantly increases the water solubility of the phenylborate group.[49] Based on the change in charge property, hydrophilicity and hydrophobicity, and the specific combination between the phenylboronic group and hydroxyl groups (on the carbon in positions 1 and 2, and carbon in positions 4 and 5 on glucose), glucose-sensitive materials based on phenylboronic polymers can be designed. It is worth noting that while the phenylboronic group and glucose molecules form a relatively strong dynamic borate ester bond,[50–52] intermolecular hydrogen bonding and other bonding effects may exist, which make the phenylboronic group and glucose molecules form a more stable planar or three-dimensional multicomponent ring structure. Thus far, research has not confirmed this point, and accordingly this interaction needs further experimental exploration and verification.

Through the transformation of the charged properties of phenylboronic acid-based polymers, effective drug loading and release can be realized. Zhen Gu *et al.*[53] designed phenylboronic acid-based polymer segments to exhibit positive electrical characteristics in the physiological environment, which could be combined with negatively charged insulin, creating electrostatic interactions that contribute to insulin loading

(Fig. 5(a) and (b)). When the phenylboronic acid group in the polymer segment was combined with glucose, the charge of the segment changed, and the negatively charged insulin molecules were gradually repelled, released into the tissue fluid, and exhibited the effect of lowering blood glucose.

Effective drug loading and release can be achieved through the hydrophilic–hydrophobic transition of phenylboronic acid-based polymers. As shown in Fig. 5(c) and (d), Yeu-Chun Kim *et al.*[54] prepared an amphiphilic polymer segment containing a hydrophobic phenylboronic acid group and a hydrophilic amino group. It could be self-assembly into polymeric vesicles in solution. Insulin was encapsulated in the vesicles. When glucose entered the vesicles and combined with the phenylboronic acid groups, the hydrophobic environment in the vesicle changed, causing the vesicles to expand or dissociate, leading to the release of insulin. Similarly, the particle models of the same glucose-sensitive mechanism can be roughly divided into micelles, vesicles, and liposomes.

The strategy of using glucose as a dynamic exchange substance to replace the binding points formed by polymers based on phenyl borate and other diol structures can also be used to establish glucose-responsive drug delivery models based on dynamic gel networks. Xiang Chen *et al.*[55] grafted
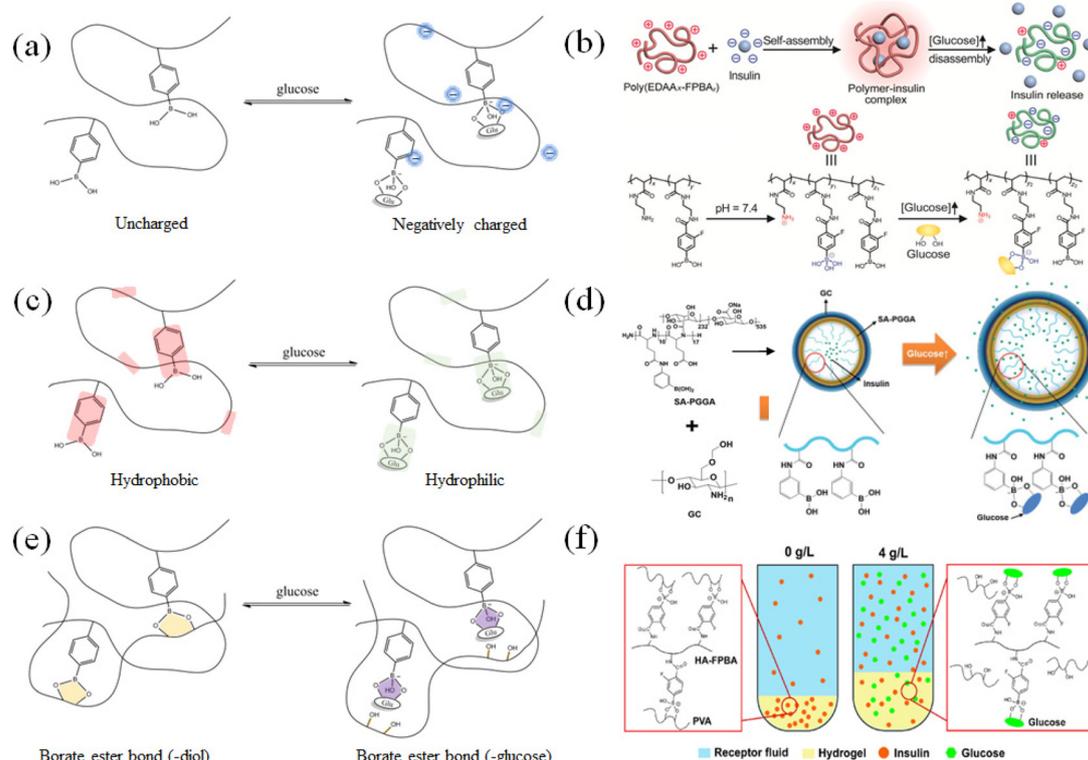

Fig. 5 Glucose-sensitive model of phenylboronic acid-based polymers. (a) and (b) After the phenylboronic acid group binds to glucose, the charge of the polymer segment changes. (Adapted with permission from ref. 53. Copyright © 2019, The Authors, some rights reserved, exclusive licensee American Association for the Advancement of Science.) (c) and (d) Glucose is combined with phenylboronic acid groups to improve their hydrophilicity. (Adapted with permission from ref. 54. Copyright © 2019, The Authors, some rights reserved, exclusive licensee American Association for the Advancement of Science.) (e) and (f) Glucose-substituted diol structure binds to phenylboronic acid, resulting in the disruption of the polymer cross-linked network. (Adapted with permission from ref. 55. Copyright © 2021 Wiley-VCH GmbH.).

phenylboronic acid groups on polyallylamine segments and mixed them with polyvinyl alcohol to prepare gels (Fig. 5(e) and (f)). The phenylboronic acid group combined with the diol structure on the polyvinyl alcohol to form a relatively stable gel network as a cross-linking point. When the gel was placed in a high-concentration glucose solution, the glucose molecule replaced the original borate ester bond and generated a new structure with the phenylboronic acid group. Consequently, the gel network was disrupted to swell or dissociate, and then insulin was released. A small molecule containing a phenylboronic acid group could also be used as a cross-linking agent to prepare a polymer network structure, which could be loaded with insulin, and under the specific substitution of glucose, glucose-sensitive release could be accomplished. Generally, based on this response mechanism, various types of gel networks can be designed.

The pK_a of phenylboronic acid is 8.8–8.9, which is higher than physiological pH,[56] making it easy to aggregate *in vivo*, and thus limiting the binding ability of the phenylboronic acid group to glucose molecules to a certain extent.[57] However, the structure of phenylboronic acid-based polymers can be modified to improve their glucose-sensitive properties.[58] In addition, there are issues with drug inactivation and inadequate drug loading during the preparation of phenylboronic acid-based GSMSs and the loading process. The risk of drug inactivation can be reduced by choosing a relatively mild preparation and storage environment. In drug delivery based on common mixing, the loading capacity of the drug can be improved by means of electrostatic interaction.

The function of glucose-responsive substances in GSMSs is to recognize changes in the blood glucose concentration and regulate the efficiency of insulin release in real time. At the beginning of treatment, if the microneedles do not contain glucose-sensitive substances, it may lead to the sudden release of insulin. GSMSs, which contain glucose-sensitive substances, may protect against the risk of hypoglycemia to some extent. Meanwhile, when the blood glucose returns to the normal range, glucose-sensitive substances are needed to recognize the decrease in blood glucose, and thus reduce the drug release. Moreover, GSMSs are required to recognize and control the drug release rate when the blood glucose changes again due to eating. In conclusion, GSMSs need to have a good glucose response function and maintain a relatively persistent and repeated glucose gradient-response characteristic.

3.2. Preparation of glucose-sensitive models based on glucose oxidase (GOx) and their response characteristics

The proportion of β-D-glucose, α-D-glucose and linear glucose in the blood is about 63%, 33%, and 1%, respectively, and there is a dynamic transformation balance among the different types of glucose. Scheme 2 illustrates that glucose oxidase can change glucose into hydrogen peroxide and gluconic acid.[59] GOx can quickly identify glucose molecules and consume oxygen to convert them into gluconic acid, which can create a local acidic environment and generate hydrogen peroxide molecules with strong oxidative properties (Fig. 6(a)).
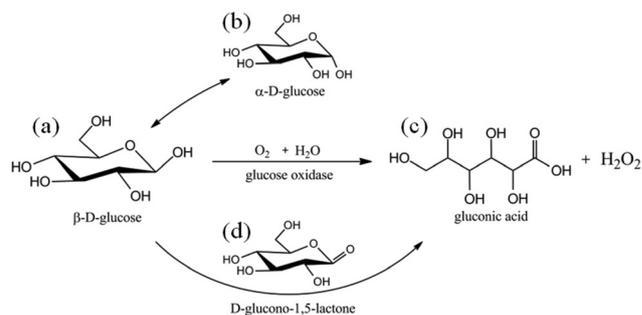
Scheme 2 Schematic diagram of glucose oxidase catalyzing glucose.

During this process, the changes in the microenvironment before and after transformation can be used to design glucose-sensitive models.

The catalytic action of GOx can convert glucose into gluconic acid and hydrogen peroxide.[60] The response model is designed through the acidic environment generated by catalysis, such as electrostatic interaction, host–guest interaction, and hydrophilic–hydrophobic transition. As shown in Fig. 6(b), Omar Azzaroni *et al.*[61] prepared a cross-linked polymer network with positively charged amino groups, and simultaneously loaded insulin and glucose oxidase. The local acidic microenvironment caused amino protonation in the polymer segment, which destroyed the previously tight cross-linking network, thus realizing the glucose-sensitive release of insulin.

After glucose is oxidized by the enzyme, the produced hydrogen peroxide can also be used to design a glucose-sensitive model through the redox mechanism. Katsuhiko Sato *et al.*[62] prepared polymersomes containing glucose oxidase and phenylboronic acid groups (Fig. 6(c)). The generated hydrogen peroxide could oxidize the borate ester bond, causing the shell structure of the vesicle to cleave and release the drug. The strong oxidizing properties of hydrogen peroxide could realize a variety of response phenomena. However, due to the potential damage risk of GOx to human cells and tissues, the accuracy of GOx dosage and the by-products from the catalytic process need to be specially considered when designing the glucose-sensitive model based on glucose oxidase. As shown in Fig. 6(d), Yanqi Ye *et al.*[17] designed and fabricated a glucose-sensitive model of GSA containing multiple enzymes. In the hypoxic environment, GSA would rapidly dissociate and lead to insulin release. Glucose diffuses through microneedles and interacts with cells encapsulated in alginate micro gel to promote insulin secretion. GSA is a self-assembled polymer nanovesicle containing three enzymes, *i.e.*, glucose oxidase, α-amylase and glucoamylase. Once affected by elevated blood glucose, GSA (composed of anoxic-sensitive substances) rapidly dissociates and releases encapsulated enzymes in response to glucose oxidation and oxygen consumption.

The biggest challenge associated with GSMSs based on glucose oxidase is the enzymatic inactivation caused by the decrease in local oxygen concentration, pH changes and internal microenvironment during the reaction. Meanwhile,
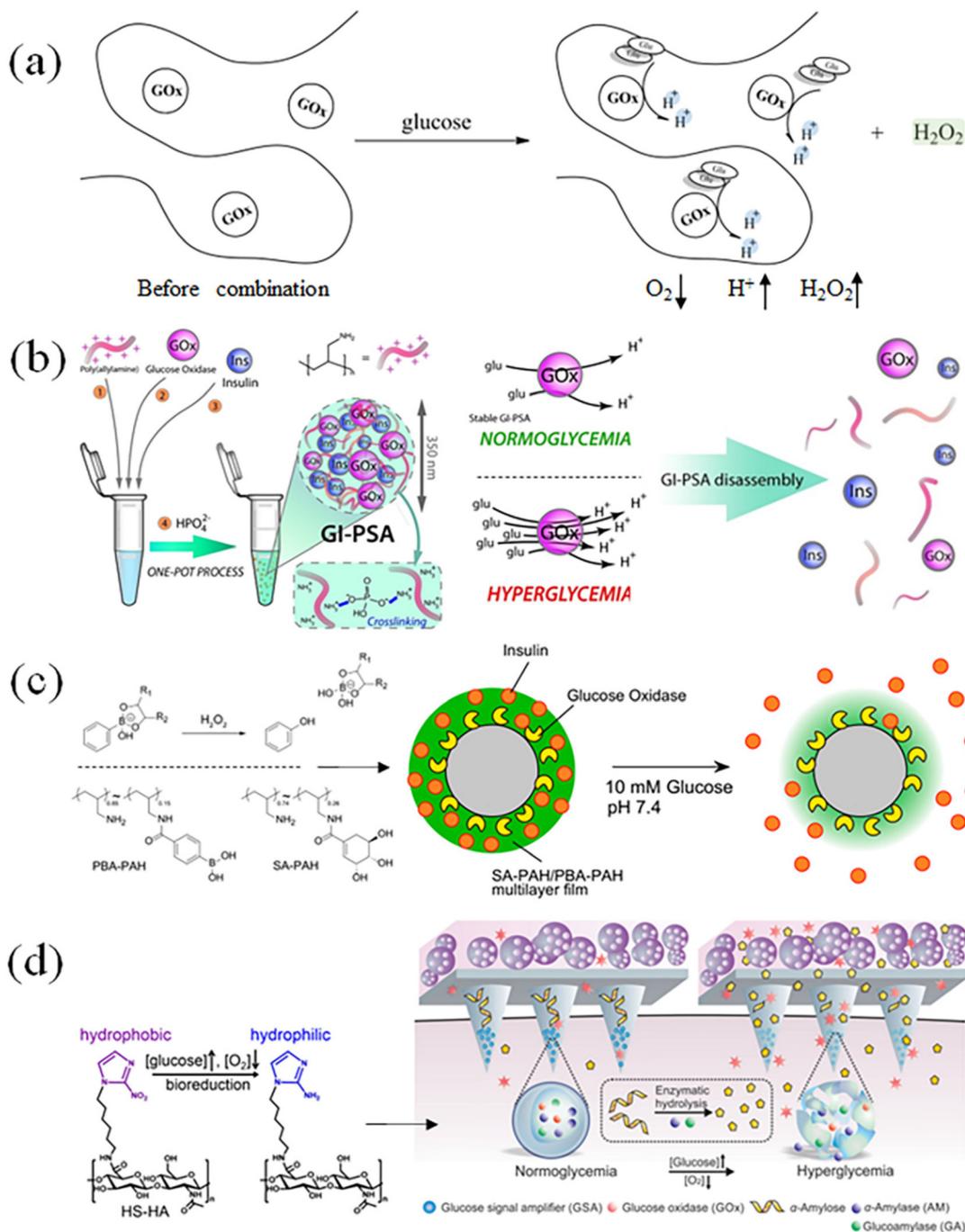
Fig. 6 Glucose-sensitive model of GOx with polymers. (a) and (b) Glucose oxidase converts glucose into gluconic acid and hydrogen peroxide and causes electrostatic repulsion of polymer segments through protonation. (Adapted with permission from ref. 61. Copyright © 2019, Wiley-VCH Verlag GmbH & Co. KGaA, Weinheim.) (c) Acidic environment brought by gluconic acid can be used in acid–base reactions or host–guest inter-actions. (Adapted with permission from ref. 62. Copyright © 2018, Multidisciplinary Digital Publishing Institute.) (d) Increased concentration of hydro-gen peroxide, which utilizes its oxidative properties to disintegrate polymer gels or particles. (Adapted with permission from ref. 17. Copyright © 2016, WILEY-VCH Verlag GmbH & Co. KGaA, Weinheim.).

tissue inflammation, which may be caused by hydrogen per-oxide, is also another important issue in these systems,[63–65] and the addition of catalase (CAT) is the most commonly used strategy.[66,67] However, the oxidation of glucose oxidase will consume oxygen, which may potentially affect the activity state of the surrounding cells and tissue,[68–70] and the gluconic acid

produced after the reaction makes the local environment acidic,[71–73] also causing a disturbance in the body due to a short time of homeostasis. Therefore, using glucose oxidase as a glucose-responsive substance has obvious disadvantages. The security risks generated in the response also limit their application scope.

3.3. Preparation of glucose-sensitive models based on concanavalin A (Con A) and their response characteristics

In the state of the active tetramer, concanavalin A has four sites that can form specific binding with glucose (Scheme 3).[74–76] The combination of concanavalin A and glucose satisfies the fast and specific characteristics, and thus is also used to design a type of glucose-sensitive material.

As shown in Fig. 7(b), Weitai Wu *et al.*[77] combined concanavalin A with polymer segments and formed a cross-linked agglomerate structure, and the specific binding of glucose to Con A resulted in the expansion of the cross-linked network and promoted drug release. The design of the crosslink density could achieve rapid response to different concentrations of glucose. Jun Nie *et al.*[78] designed a polymer network with Con A as a cross-linking agent, which could simultaneously respond to pH and glucose (Fig. 7(d)). When the gel was placed in a high-glucose concentration environment, the glucose combined with Con A, destroying the original gel network and dissociating it to complete the drug release.
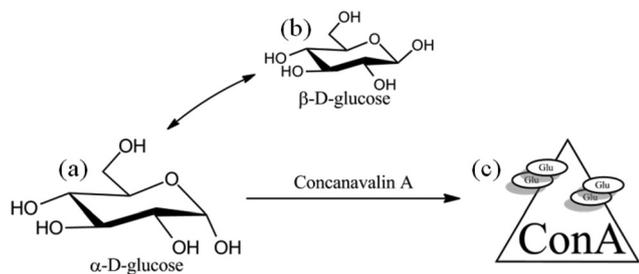
Concanavalin A-based glucose-sensitive systems currently have some limitations, including toxicity, poor water solubility[79] and stability,[80] and longer glucose-sensitive response time.[81] Although it can be improved by modification with hydrophilic polymers, the immunogenicity of Con A still needs to be addressed. In addition, the environmental differences and the changes in the substance itself brought about by Con A before and after combining with glucose still need to be further explored and studied.

4. Regulation of blood glucose with GSMSs based on glucose-sensitive models with phenylboronic acid

The advantages of phenylboronic acid-based GSMSs include low cost, absence of immunogenicity, high versatility, and good *in vivo* stability.[70–72] Compared with GOx and Con A, phenylboronic acid-based polymers are a better choice for the design of glucose-sensitive models.

Phenylboronic acid-based polymer GSMSs are made up of a microneedle body, glucose-regulating medication, and glucose-sensitive model. Designing the structure and collocation of polymers based on phenylboronic acid allows for the establishment of glucose-sensitive models. The glucose-sensitive models based on phenylboronic acid can be subdivided into three categories, *i.e.*, the gel model, particle model, and composite structure model. We compared and examined the features of each model and the corresponding controlled drug-release mechanism. Meanwhile, the characteristics and operating principles of three classes of glucose-controlling medications were examined, and the benefits and drawbacks of various loading strategies for the drugs were investigated. Finally, the preparation of microneedles and microneedle materials, as well as the performance characterization and analysis of the microneedles were discussed. The interaction and equilibrium relationship among the three components, as

Scheme 3 Schematic diagram of the binding between concanavalin A and glucose.
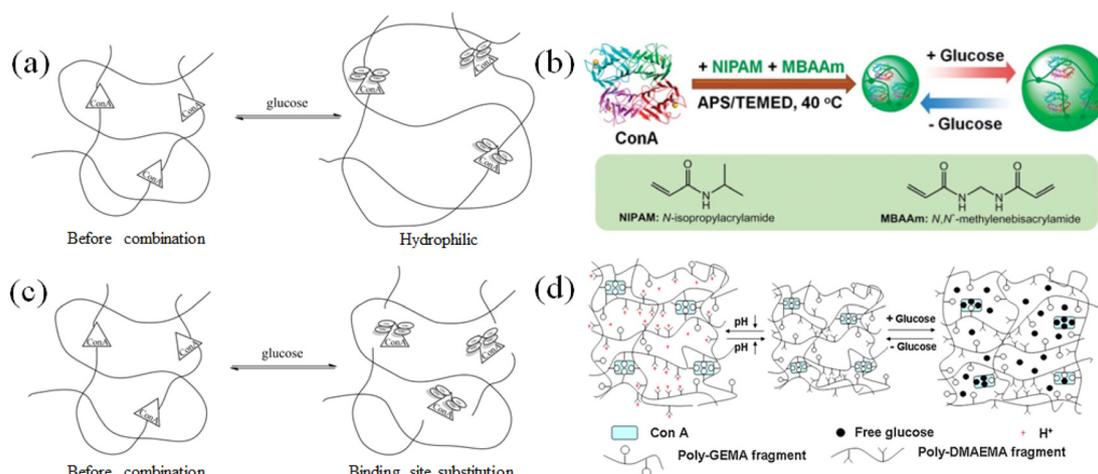

Fig. 7 Glucose-sensitive model of Con A-based polymers. (a) and (b) Concanavalin A binds to glucose, which increases the steric hindrance and swells the cross-linked network. (Adapted with permission from ref. 77. Copyright © 2015, The Royal Society of Chemistry.) (c) and (d) Concanavalin A specifically binds to glucose, replaces the cross-linking point, and disintegrates the integrity of the cross-linking network. (Adapted with permission from ref. 78. Copyright © 2011, Elsevier B.V. All rights reserved.).

well as the application prospect and improvement scheme of phenylboronic acid-based GSMS were explored.

4.1. Microneedle body in GSMSs

The primary function of the microneedle body is loading and delivering medications and glucose-sensitive models. Therefore, the body of the microneedle needs to be capable of storing drugs and have sufficient quality, adequate mechanical strength and weather resistance. The safety of microneedle therapy, the drug release effect, and the controllability of the release are all impacted by the composition and structure of the microneedle body.

4.1.1. Selection of materials and classification of microneedle system. The main body material of the microneedle needs to provide sufficient ability to penetrate the skin epidermis and deliver the drug to the dermis during the treatment of diabetes. As the outermost protective carrier and transmission medium of drugs, the mechanical strength of the needle material and structure required for treatment are the primary conditions.[82] Secondly, according to the properties of the drug, such as the active environment and time, it is very important to select the needle material and structure suitable for long-term drug storage and drug release.[83,84] In addition, given that the drugs are released in the dermis layer of the skin, they will come into contact with cells and peripheral tissues. In addition, because the microneedle releases drugs in the dermis, the safety of the materials used for cells and surrounding tissues is also particularly important.[85]

The morphological changes before and after the microneedle delivers the drug can be used to categorize the microneedle bodies into two groups. One type of microneedle is insoluble,

while the other type is soluble (Fig. 8). The term "insoluble microneedle" refers to a needle body that maintains its original state following transdermal drug delivery, *i.e.*, the primary function of the microneedle is to create a drug delivery channel on the skin. This type of microneedle is frequently made from both metallic and inorganic non-metallic materials to achieve its primary effective skin piercing performance. However, due to the resistance and friction of the surface layer of the skin, needle material loss and chipping can occur during piercing. Consequently, localized inflammation will occur due to the body's immune response if these tiny material fragments are not removed from the skin and tissues in a timely manner.[86,87]

The soluble microneedle refers to the dissociation of the microneedle body through dissolution, swelling, degradation and other means after the microneedle body is implanted in the skin to release the drug. This type of microneedle usually uses organic materials as the main body or a combination of organic and inorganic materials. After the organic materials undergo polymerization, cross-linking, doping, freezing and other processing methods, they can achieve better mechanical strength and higher skin penetration.[88–90] The unique biocompatibility of some organic materials also reduces the toxicity and immune rejection of the body caused by the transdermal administration of the needle material during use.

Compared with soluble microneedles, insoluble microneedles also show the benefits of therapeutic manipulation in accelerating healing. Implantation and extraction are the two basic steps in the treatment using insoluble microneedles. The drug is usually stored in the microneedle or coated on its surface.
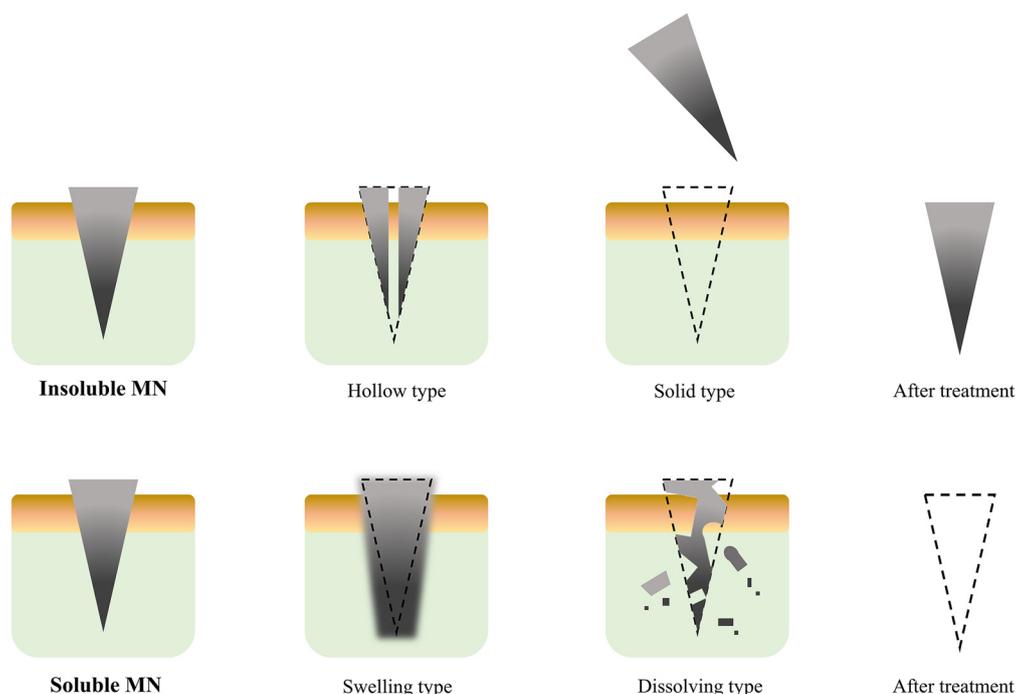

Fig. 8 Classification of microneedle system: insoluble type and soluble type.

After the needle is removed, it is applied to the skin. This drug delivery method may have problems such as low drug loading, laborious loading steps and difficult operation. However, soluble microneedles can relatively increase the drug loading, better protect drug activity, and minimize unnecessary drug waste, which improves treatment compliance and convenience.

4.1.2. Preparation of polymeric microneedle system. The selection and preparation of polymer microneedle materials have a direct impact on the fundamental questions of mechanical strength of the microneedle, drug loading strategy, toxicology, and biocompatibility. Polymeric microneedles are usually fabricated by molding.[91] The steps include adding a precursor solution or gel to the master mold, shaping the microneedle structure by processing methods such as centrifugation and vacuum drying, and finally demolding to complete the preparation of the microneedle. Microneedles can also be prepared by 3D printing,[88] where the polymer raw materials are added to the 3D printer, extruded by heating, and then a mold it used to stretch and shape the polymer (Fig. 9). Earlier, microneedles were prepared *via* hot pressing and extrusion, and then stretching.[92]

Compared to other microneedle preparation techniques, the molding method has relatively simple operational steps and makes it easy to incorporate drugs. The preparation time of each microneedle may vary from several minutes to hours.

Therefore, the challenges to be solved before the large-scale industrial production of microneedles include increasing their output and simplifying the manufacturing process and steps.

The materials and specifications used to prepare microneedles over the last three years are listed in Table 1. The biocompatibility and mechanical strength of microneedles are directly influenced by their materials. Polyvinyl alcohol and polyvinylpyrrolidone are used as the base for microneedles. Meanwhile, lactic acid, polyglycolic acid, and other bases have also been used to make microneedles. These artificial polymers have the mechanical strength required for skin penetration by microneedles. In addition, natural polymers are also used to prepare microneedles, *e.g.*, polysaccharides, amino acids, and proteins, while chitosan, gelatin, lysine, and silk fibroin are some of the commonly used substrates. Because of their good biocompatibility, these natural polymers can reduce the immune response to microneedle therapy and improve the safety of treatment.

4.1.3. The shape and arrangement of the microneedle system. Microneedles penetrate the skin surface, opening a channel for drug transmission. The height, bottom, distance and surface area of the microneedle all determine its therapeutic effect. The height of the microneedle affects the depth of drug release. The distance between the needle body and the bottom determines the drug loading and local release density

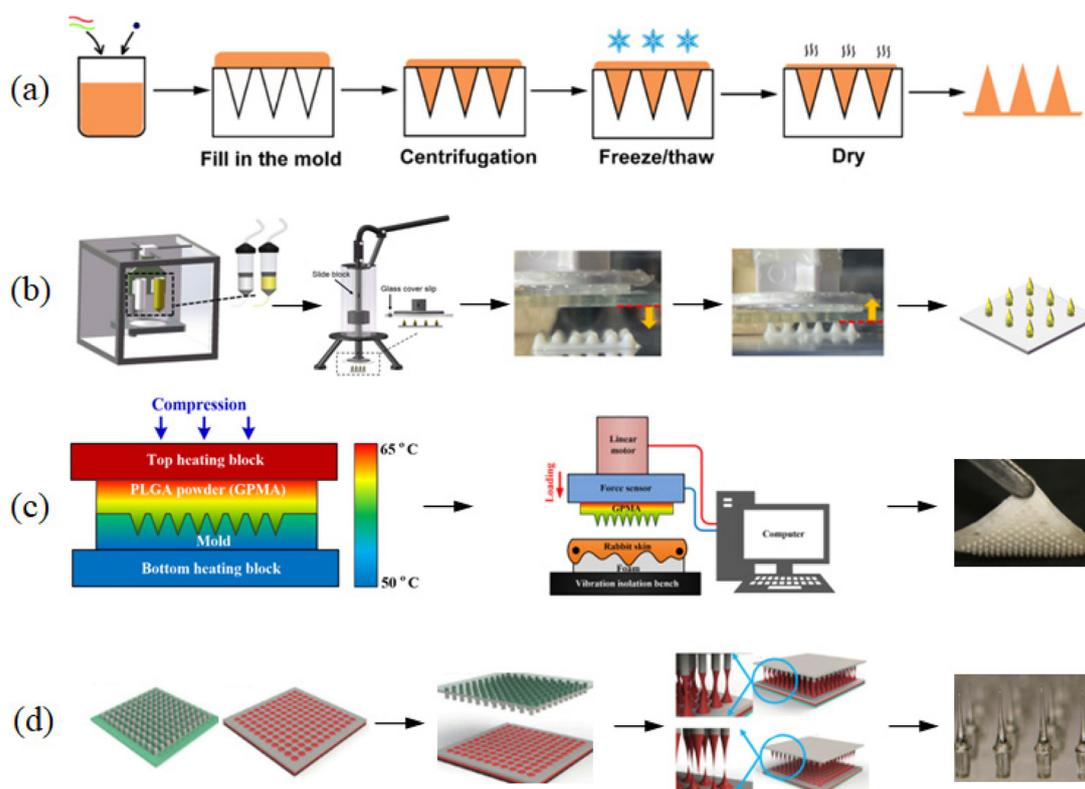Fig. 9 Method for the preparation of microneedles. (a) Molding. (Adapted with permission from ref. 91. Copyright © 2021, the American Chemical Society.) (b) 3D printing. (Adapted with permission from ref. 88. Copyright © 2020, Elsevier B.V. All rights reserved.) (c) Hot pressing. (Adapted with permission from ref. 92. Copyright © 2019, Elsevier B.V. All rights reserved.) (d) Extrusion stretching.[93] Copyright © 2015, IOP science.

Table 1 Main materials, microneedle size, loaded drugs, and drug loading reported in the past three years

| Needle material | Loaded drug | The size and arrangement of microneedle and patch | | | | | | Performance of microneedle | | |
		Height (µm)	Base width (µm)	Tip width (µm)	Interval distance (µm)	Quantity	Area (cm^2)	Failure force (N/patch)	Drug loading	Ref.
Hyaluronic acid	Insulin	500	200			15 × 15		0.137		57
Polyvinyl alcohol, sucrose	Insulin	750	300	20	500	10 × 10	0.25	0.2		94
Polyvinylpyrrolidone K29/32	Lixisenatide	600				15 × 15	0.64		4.25 µg per patch	95
Polyvinyl alcohol, folic acid	Insulin	532	277		167		0.5		10.54 µg per patch	96
Polycarbonate	Insulin	1000	500				0.44		3.20 mg per patch	97
Hyaluronic acid	Insulin	600	300			10 × 10		0.45		98
Polyethylene glucosel, ethoxylated trimethylolpropane triacrylate	Insulin	860	360			10 × 10		0.3	0.6 IU per patch	99
Gelatin methacryloyl	Metformin	600	200		500	10 × 10		1.2		100
Poly(vinyl pyrolidone), tartaric acid	Metformin	750	250		450	10 × 10	0.25	0.1–0.15		101
Polyvinyl alcohol	Metformin	600	200			15 × 15	1	0.176		102
Polyvinyl alcohol	Insulin	600	120			7 × 7			3.99 mg per patch	103
Silk fibroin	Insulin	600	330			15 × 15			5 IU per patch	104
Polyvinyl alcohol, polyvinylpyrrolidone	Insulin	750	300			10 × 10				105
Pullulan	Insulin	550	200	500		15 × 15	0.64	0.3		106
Pullulan	Insulin	600	300	150		19 × 19	0.49			107
Sodium alginate, hydroxyapatite	Insulin	643	601	24		6 × 6	0.44			108
Silk Fibroin	Insulin	500				15 × 15		0.5	1.25 mg per patch	109
Silk Fibroin	Insulin	700				10 × 10	0.64	0.74		110

(Fig. 10). This structure also affects the effectiveness of drug delivery and treatment results.

The fracture strength and puncture effectiveness of the microneedle will be influenced by its geometry. The microneedle array in Fig. 10(a, c, and e) consists of conical and pyramidal needle bodies, which are usually prepared *via* the template method. The conical and pyramidal microneedles have the best penetration effect according to theoretical analysis and
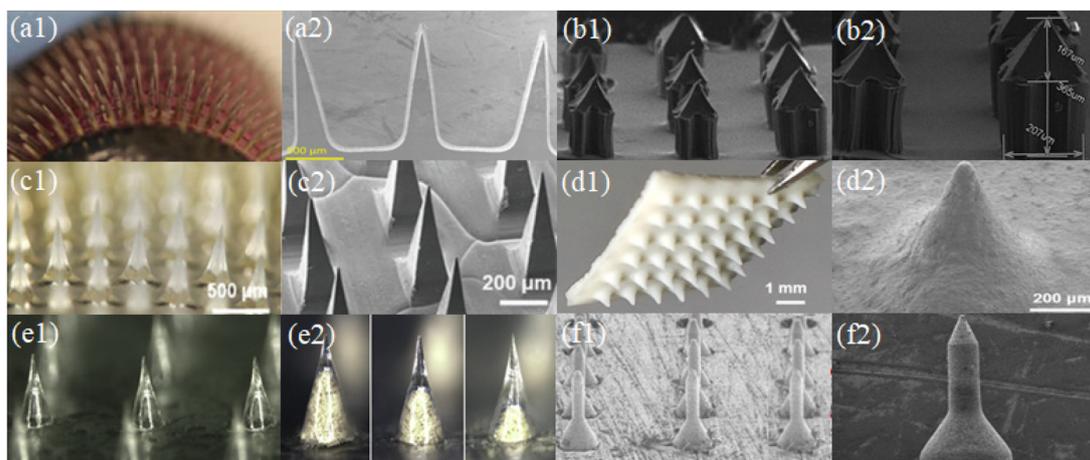

Fig. 10 Arrangement of microneedle system (a1–f1) and shape of microneedle (a2–f2). (Adapted with permission from ref. 111. Copyright © 2014, Taylor & Francis Online.) (Adapted with permission from ref. 96. Copyright © 2022, WILEY-VCH Verlag GmbH & Co. KGaA, Weinheim.) (Adapted with permission from ref. 88. Copyright © 2020, The Author(s), under exclusive licence to Springer-Verlag GmbH, DE part of Springer Nature.) (Adapted with permission from ref. 112. Copyright © 2020, Elsevier Ltd. All rights reserved.) (Adapted with permission from ref. 104. Copyright © 2020, Multidisciplinary Digital Publishing Institute.).

practical testing. These two microneedle morphologies are the most frequently used microneedle models and experience the least resistance during skin implantation. The array of microneedles in Fig. 10(b, d, and f) consists of either a multi-stage structure or one-piece structure. These microneedles can be created by 3D printing or laser cutting casting. Specific structural designs are often applied for specific therapeutic needs. For example, different skin microneedles have different epidermal layers of different thickness, requiring longer and harder microneedles, or requirements for the depth of drug delivery and layered delivery of multiple drugs.

4.1.4. Evaluation of the puncture pain, biocompatibility, and mechanical strength of microneedle system. The material and structure of the microneedle body and the placement of the microneedle patches have an impact on the ability of the microneedle to pierce. The difficulty of forming and processing microneedles and their mechanical strength following shaping are both influenced by the intermolecular force in the needle body material. The mechanical strength of a single microneedle body is determined by the smoothness of the structure and morphology of the needle body. The overall piercing effect of the microneedle patch is determined by the number and how the needles are arranged. A microneedle body with a length between 500 and 1200 μm has a good punc-

ture effect and will not result in overt pain or trauma according to research on the human epidermis.

For the analysis of the mechanical strength of microneedles, a compression test on the microneedle is usually performed using a universal material testing machine. The test methods can be divided into two categories. As shown in Fig. 11(a), the microneedle is placed on pigskin and a vertical compressive force is applied to the microneedle and pigskin as a whole. A clear inflection point was observed during the test, confirming the successful puncture of the microneedle pigskin under this pressure and overall longitudinal deformation.[113] The second category shown in Fig. 11(b) is the compression test that only applies vertical pressure on the top and bottom of the microneedle. The resulting curves were longitudinal microneedle deformation *versus* pressure. These test curves were usually smooth, and if there were turning points, there may be brittle fractures caused by the compression of the microneedle.[114] The actual deformation degree of the microneedle under different pressure loads and various types of variables is shown in more detail (Fig. 11(c)). With an increase in the compressive load in the vertical direction, the bending deformation of the microneedle also gradually increased. This type of microneedle had good toughness, and thus the microneedle maintained a good finish before and
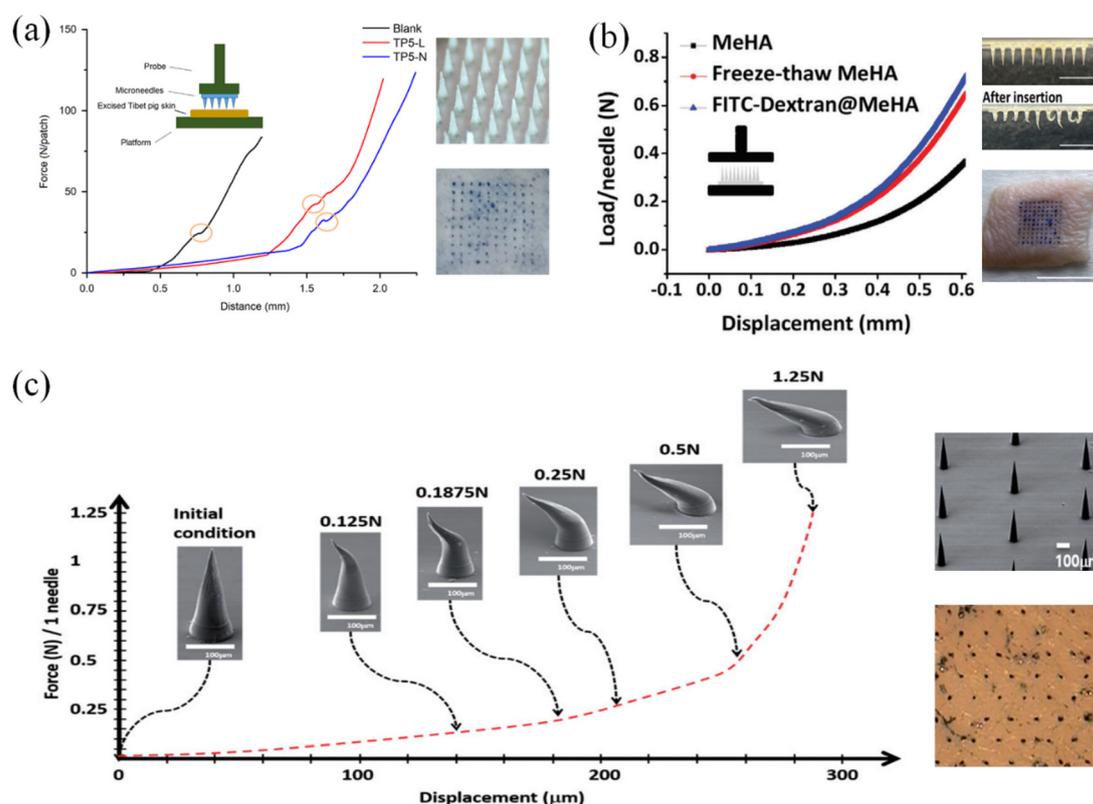

Fig. 11 (a) Compression test of microneedle and pierced pigskin. (Adapted with permission from ref. 113. Copyright © 2018, Chinese Pharmaceutical Association and Institute of Materia Medica, Chinese Academy of Medical Sciences. Production and hosting by Elsevier B.V.) (b) Compression test of microneedle body. (Adapted with permission from ref. 114. Copyright © 2020, WILEY-VCH Verlag GmbH & Co. KGaA, Weinheim.) (c) Real morphology of microneedles under different pressure and deformation degree tests. (Adapted with permission from ref. 115. Copyright © 2018, Taylor & Francis Online.).

after treatment.[115] Meanwhile, it could reduce inflammation of the skin epidermis due to residual material debris.

Moreover, it has been confirmed by experiments that when the deformation degree of a single needle body was 300 microns and the pressure reached 0.02 N,[116] it could successfully penetrate the skin epidermis. The conical structure of the neat microneedle array also had better skin penetration efficiency.[117] However, due to different designs, the microneedle lengths, arrangement and number of microneedles in the literature are different, and the actual puncture test results on animal skin should be used as a reference. Also, due to the difference in the composition and thickness of the stratum corneum, it is necessary to design microneedles according to the injection site to achieve the required strength.

The biosafety test of microneedles is one of the important inspection indicators before their application. The biocompatibility of the microneedle material determines the immune response and toxicity of the puncture treatment. The biocompatibility and safety of materials can be directly investigated through *in vivo* experiments. As shown in Fig. 12(a), a microneedle was applied to the back of a mouse, and the number of pinholes on the skin surface after the removal of the microneedle was examined. The living biological epidermis has good self-healing ability. Through the analysis of the microneedle wound, it was shown that the microneedle caused slight damage and the body could achieve rapid self-healing.[118] The analysis of the tissue sections at the treatment site and the number and distribution of neutrophils and lymphocytes indicated that there would be mild inflam-
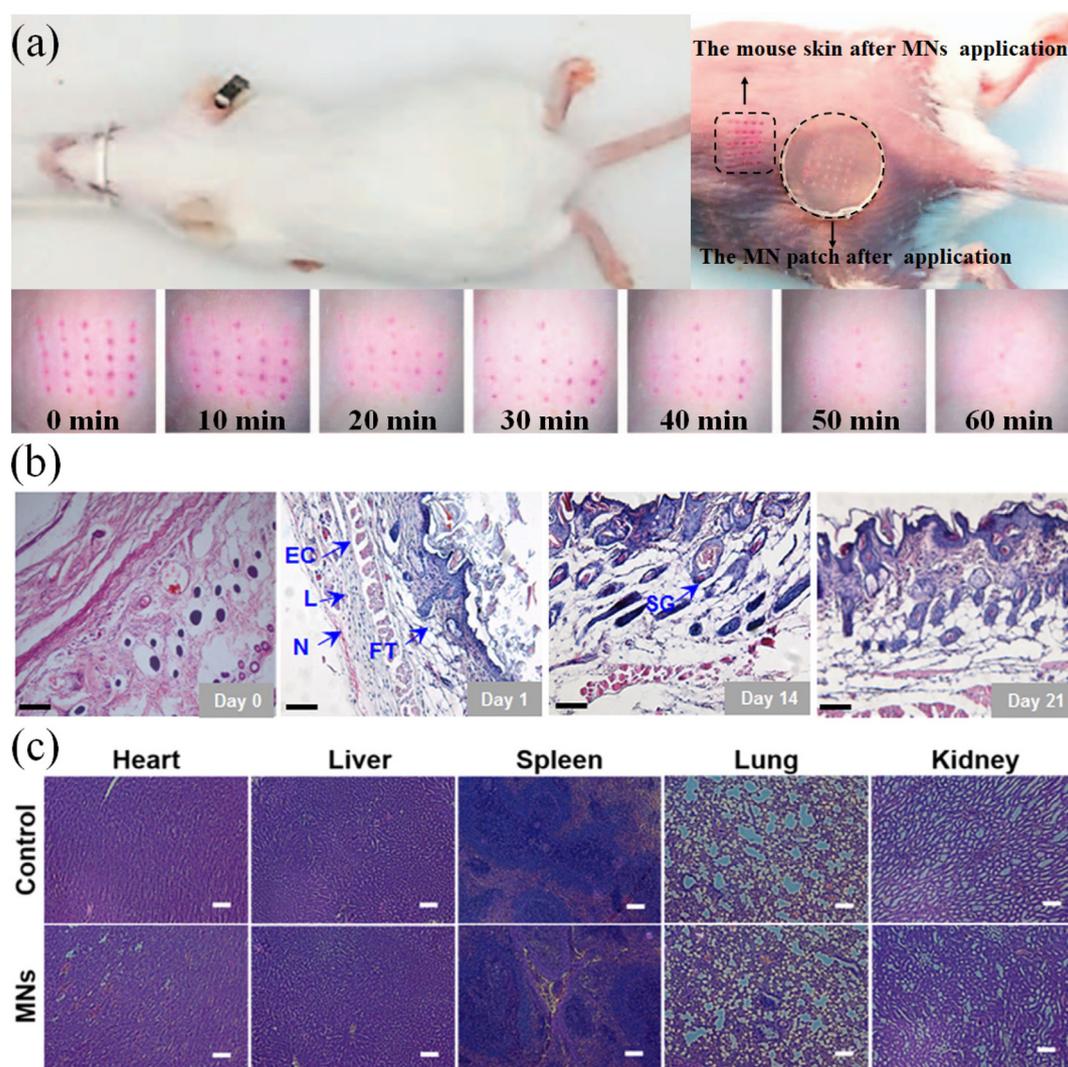

Fig. 12 (a) Skin recovery of mice within 0–60 min after microneedling treatment. (Adapted with permission from ref. 118. Copyright © 2017, Elsevier B.V. All rights reserved.) (b) Inflammation of skin sections from the microneedle-treated area within 21 days (L: Lymphocyte, N: Neutrocyte, FT: Fibrous tissues, EC: Epithelial cell, and SG: Sebaceous gland). (Adapted with permission from ref. 119. Copyright © 2021, American Pharmacists Association. Published by Elsevier Inc. All rights reserved.) (c) H&E stained images of major organs after treatment with MNs and the untreated samples as a control group. (Adapted with permission from ref. 120. Copyright © 2017, Acta Materialia Inc. Published by Elsevier Ltd. All rights reserved.).

mation within two weeks after the microneedle treatment (Fig. 12(b)). After three weeks, the body returned to normal levels.[119] Also, the possible rejection phenomenon in the body after microneedle treatment was explored by comparing tissue sections of diverse organs (Fig. 12(c)).[120]

The degree of pain in the puncture of microneedle therapy is another important indicator before its application. As depicted in Fig. 13(a–c), the arms, abdomen and forehead were selected as experimental sites to record and analyze the pain in the human body. The length and overall arrangement of the microneedles are important variables that produce different sensations. Longer microneedles and denser arrangements may result in a more pronounced puncture sensation. The degree of pain was very mild and difficult to detect.[121] The pain test by microneedle puncture was performed on 100 volunteers using the visual analog pain assessment method (Fig. 13(d)). The differences in pain sensation between the skin and the oral cavity were compared, and the painless and mild sensation characteristics of the microneedle treatment were summarized.[83]

4.2. Diabetes medications in GSMSs

Blood glucose is controlled by diabetic medications in GSMSs. Drugs that lower blood glucose levels and maintain blood glucose stability, such as insulin, are delivered to the dermis through the transport and protection of the microneedle. The therapeutic substance can be released from the matrix supported by polymers and diffused in the interstitial fluid under the control of glucose-sensitive models. It can lower the level of glucose in the surrounding atmosphere of the human body.

4.2.1. Classification and selection of glucose control drug.
Generally, the pharmacological treatment of hyperglycemia is based on correcting the two main pathophysiological changes that lead to elevated blood glucose in humans, namely, insulin resistance and impaired insulin secretion.[122–124] According to different types of diabetes and individual differences, the commonly used treatment drugs for diabetes can be divided into three categories (Fig. 14), i.e., oral hypoglycemic drugs (metformin as an example),[125] injectable insulin, and glucagon-like peptide-1 receptor agonists (GLP-1RA) (exenatide as an example).[126]
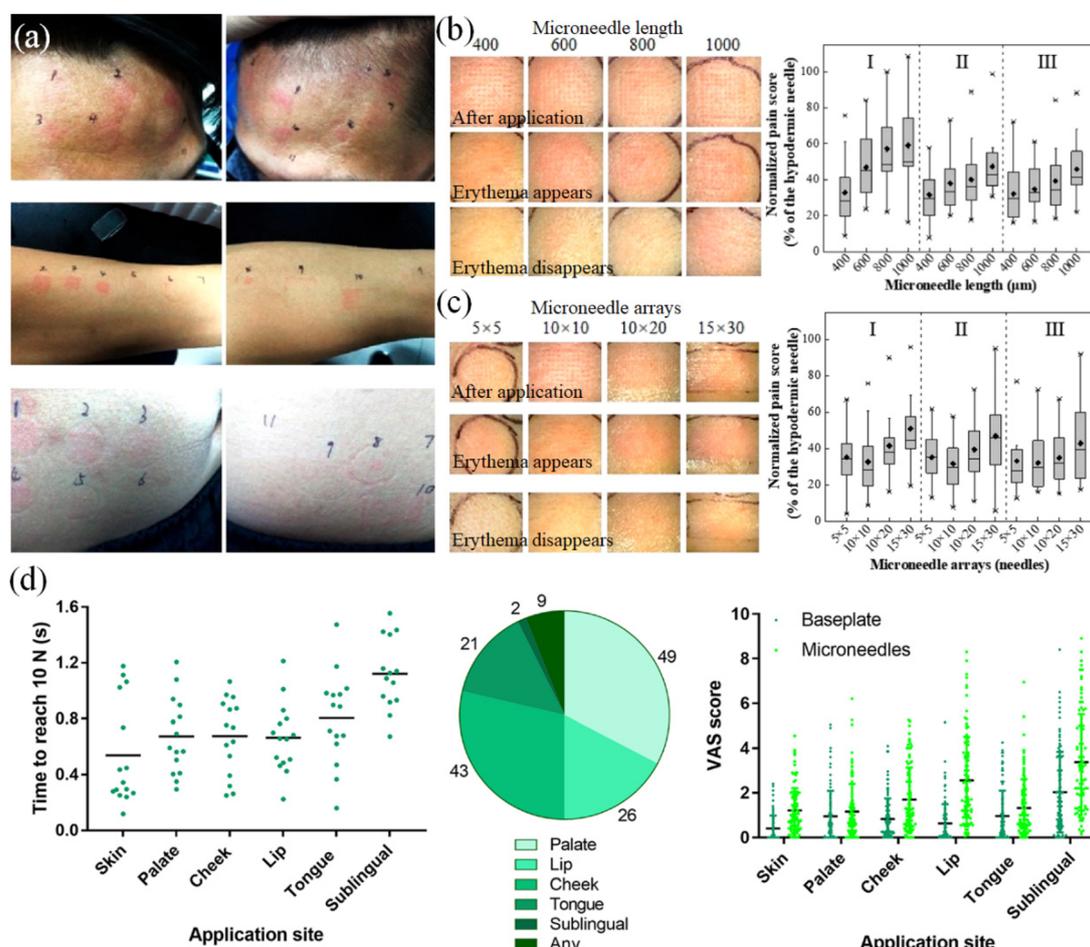

Fig. 13 (a) Effect of microneedle on the forehead, forearm and abdomen of the human body. (b) Effect of needle length on erythema and pain sensation. (c) Effect of microneedle array on erythema and pain sensation. (Adapted with permission from ref. 121. Copyright © 2019, the American Chemical Society.) (d) Microneedle at different positions pain research. (Adapted with permission from ref. 83. Copyright © 2021, The Authors, some rights reserved, exclusive licensee American Association for the Advancement of Science.).
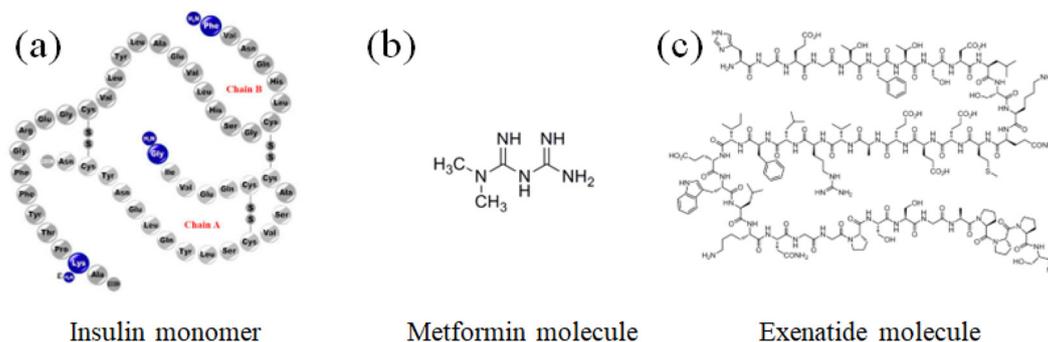
Fig. 14 Three types of hypoglycemic drugs. (a) Insulin,[125] (b) metformin,[125] and (c) exenatide.[125] Image from "Exenatide Monograph for Professionals". Drugs.com. American Society of Health-System Pharmacists. Retrieved 22 March 2019.

The main effect of oral hypoglycemic drugs is to promote insulin secretion or reduce the production of glucose in the blood *via* other mechanisms. The commonly used oral drugs include metformin, sulfonylureas, glinides, TZD, and α-glucosidase inhibitors. Taking metformin as an example, its main pharmacological effect is to reduce the blood glucose by inhibiting hepatic gluconeogenesis, reducing the output of glucose in the liver and improving the insulin resistance of peripheral tissues. It can increase the utilization of glucose by non-insulin-dependent tissues, such as the brain, intestine, and renal medulla.[127–129] Metformin does not promote fat synthesis and has no obvious hypoglycemic effect on normal people. When it is applied to patients with type 2 diabetes, it usually does not cause hypoglycemia.[130–132]

Glucagon-like peptide-1 receptor agonists (GLP-1RA) stimulate insulin secretion and inhibit glucagon secretion by binding to receptors on pancreatic islet cells in a glucose concentration-dependent manner. To realize a hypoglycemic effect, it simultaneously reduces hepatic glucose synthesis and boosts glucose uptake in muscle and adipose tissue.[132,133] Some studies have shown that treatment with glucagon-like peptide-1 receptor agonists can reduce the risk of hypoglycemia and help reduce the incidence of cardiovascular and cerebrovascular complications.[134]

Insulin therapy is the most direct and significant treatment modality for controlling blood glucose.[135] Patients with type 1 diabetes need insulin therapy to stay alive and reduce the risk of insulin complications. Although patients with type 2 diabetes can produce insulin by themselves,[136] the β-cell function of the pancreatic islet is damaged in the diseased state, resulting in insufficient insulin secretion. The mechanism of action of insulin is to accelerate the consumption of glucose in the blood through the operation of glucose, reduce blood glucose and promote the synthesis of glucosegen, fat and protein.[137]

Table 2 compares the characteristics of the three distinct treatment modalities using illustrative medications. Metformin lowers blood glucose by decreasing the production of glucosegen, increasing the sensitivity of nearby tissues to insulin, and improving glucose utilization. There is no risk of hypoglycemia during treatment, and thus the pancreatic β cells are not stimulated to produce insulin. Glucagon-like

Table 2 Three types of representative drugs for the treatment of diabetes

Name	Metformin	Insulin	Exenatide
Treatment	Oral	Injection	Injection
Target of drug	Liver, peripheral tissue	Glucose in blood	Liver, pancreas, muscle and fat
Hypoglycemia risk	Low	High	Possible
Applicable patients	Type 2 diabetes	Type 1 diabetes and severe type 2	Type 2 diabetes

peptide-1 receptor agonists promote cells to produce more insulin, while also accelerating the rate at which the surrounding tissues absorb glucose. They are sensitive to the blood glucose levels, while receiving treatment and can sharply reduce the insulin levels when they are close to normal.

Insulin therapy is the most effective way of lowering blood glucose, but the problem of hypoglycemia caused by insulin overdose treatment exists. In view of different disease characteristics and treatment needs, in some cases, the three types of hypoglycemic drugs can be used in combination.[138,139]

Because insulin cannot be substituted, it is crucial to develop a controlled release drug delivery system that reduces hypoglycemia. Through the development of glucose-sensitive response models and drug-release mechanisms, GSMSs can accomplish this goal. To significantly postpone or completely avoid the hidden risks of hypoglycemia caused by insulin therapy, the load and release of insulin can be specifically controlled prior to treatment.

4.2.2. The interaction between glucose-sensitive models and insulin. The microneedle delivery system for insulin must have effective encapsulation capabilities to avoid the loss of insulin in environments with high temperatures, humidity, or direct air contact. This increases the drug load to ensure the activity of insulin medications. There are typically five different ways to combine microneedles and insulin.

The first method is direct loading (Fig. 15(e)). This type of situation often occurs in a microneedle system with a cavity or macroporous structure. Insulin powder can be directly loaded
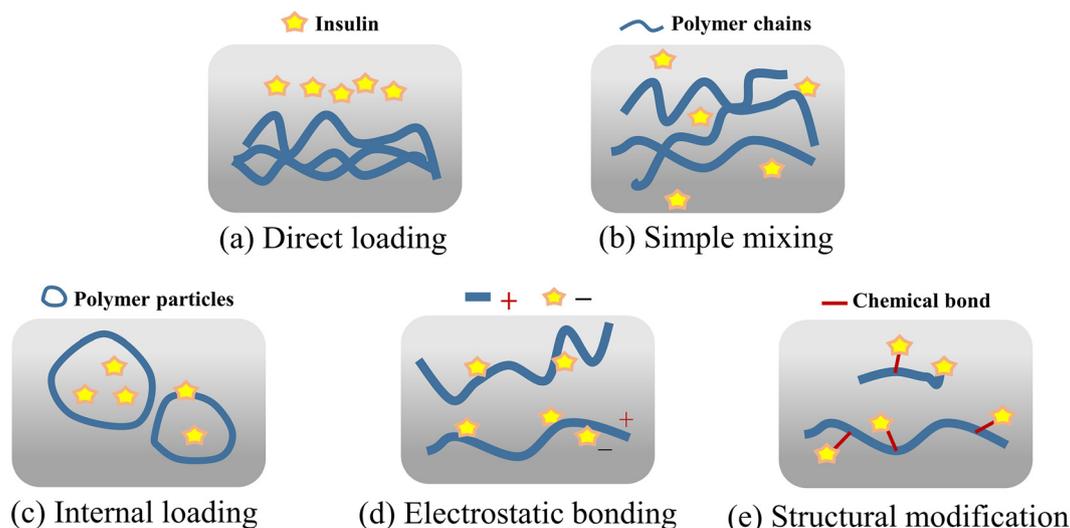
Fig. 15 Loading method of insulin in the microneedle system.

in the cavity to reduce the steps and activity loss of insulin solution during its preparation. Before insulin enters the tissue fluid, it first needs to be dissolved and diffused. A large amount of locally accumulated insulin powder may form agglomerates, and the solubility of insulin is not high in the physiological environment, which has potential for slow release and low efficacy.[105] The second is simple mixing (Fig. 15(b)). The commonly used insulin solution and polymer solution are directly mixed and used after styling and drying. The microneedle prepared by this method carries more uniformly distributed insulin and has a larger drug loading capacity. During the release of the drug, tissue fluid can quickly enter the microneedle to make it swell or dissolved, allowing the loaded insulin to be released quickly. Given that insulin is not constrained by the polymer substrate during the release, its diffusion in tissue fluid is unidirectionally accelerated and uncontrollable.[92]

The third method is internal loading (Fig. 15(c)), which commonly uses the amphiphilicity of the polymer segment to save the insulin inside the polymer particles. During drug delivery, the polymer self-assembles into a particulate structure, which has a hydrophilic part on the outside and hydrophobic part on the inside, and the polymer segments form an external protective layer for the drug, ensuring low loss and high activity during drug delivery. When the microneedle system is implanted into the skin, the polymer particles will be exposed to the tissue fluid with a high glucose concentration following the release mechanism of the microneedle system.[140] The fourth way is electrostatic binding (Fig. 15(d)). Due to the protein properties of insulin, it has charged properties in pH environments except for the isoelectric point. When paired with a polymer that also has a charged state after being ionized in a solution, loading when the polymer and insulin are attracted by the opposite charges and the release when the same charge is repelled can be achieved. Under the

influence of the electrostatic effect, stable binding and the rapid release of insulin and polymer can be achieved, and by designing the pH environment during the preparation and release, the targeted loading, rate and quantity of the region and distribution of insulin can be achieved together with its controlled release.[141]

The fifth method is a structural modification (Fig. 15(e)), which is the coupling of insulin and polymer through structural modification, and thus insulin diffuses with the movement of the polymer segments. This method reduces the free flow of insulin in the tissue fluid and improves the controllability of drug loading and the subjective regulation of the release rate.[142] However, the complexity of the preparation greatly increases and it makes it more difficult to maintain the activity of insulin.

4.2.3. The loading method of insulin as the therapeutic drug. The amount of insulin that is loaded and how easily its release can be controlled are primarily determined by the loading method (Table 3). The drug load and the utilization rate of treatment strategies are crucial to the injection treatment of diabetes mellitus. Furthermore, it is necessary to create a highly customized treatment plan for each patient, increase the drug utilization, and lessen the side effects from both inadequate and excessive doses. In addition, the composition of insulin and polymer will affect the mode of action of drugs, the way drugs are stored in microneedles, and subsequently the way drugs are released.

Table 3 Combination types of polymers and insulin

Combination type	Drug load	Release rate	Drug utilization
Direct loading	Large	Slow	Low
Simple mixing	Large	Fast	High
Internal loading	Medium	Medium	Medium
Electrostatic bonding	Medium	Fast	High
Structural modification	Small	Medium	Low

4.3. Glucose-sensitive models in the GSMS

During drug delivery, the glucose-sensitive models need to perceive and recognize changes in the blood glucose concentration, and then complete the corresponding morphological changes and control drug release. Based on this treatment, the ineffective consumption of the drug should be minimized, and the number of cycles of drug treatment should be increased (the repeated release of the drug when the blood glucose increases from high to low, to high again). Phenylboronic acid-based glucose-sensitive models can be roughly divided into three categories, including gel models, particle models, and composite structure models.

4.3.1. Preparation and glucose regulation of glucose-responsive hydrogel models. As seen in Fig. 16(a), Akira Matsumoto *et al.*[143] prepared a self-cross-linked hydrogel using MDA, AmECFPBA, and NHEAAm as raw materials, MBAAm as a cross-linking agent, and MDA and NHEAAm as amphiphilic components. The polymer segments had different ratios of hydrophilicity and hydrophobicity depending on the

feed ratio. The phenylboronic acid group present in AmECFPBA could bind to glucose and cause it to change from hydrophobic to hydrophilic. Polymer microneedles with a fixed crosslinked structure could rapidly and persistently respond to changes in glucose concentration through osmotic pressure and hydrophilic and hydrophobic conversion.[144] After being made into a microneedle and applied to high glucose levels, the hydrophilicity of the gel was significantly improved by the interaction between the phenylboronic acid group and the glucose, which caused the gel to swell and release the drug. Jicheng Yu *et al.*[141] also adopted a similar preparation method using NVP, DMAEA, and 3APBA as raw materials, and EGDMA as a cross-linking agent to prepare hydrogels (Fig. 16(b)). NVP could be used as a reactant to dissolve other monomers. Phenylboronic acid groups and positively charged DMAEA components were present in the synthesized polymer segment, which could interact electrostatically with the negatively charged insulin molecules. Moreover, the electrostatic effect can also be used as the drug release mechanism. The phenylboronic acid group exhibits negative electric character-
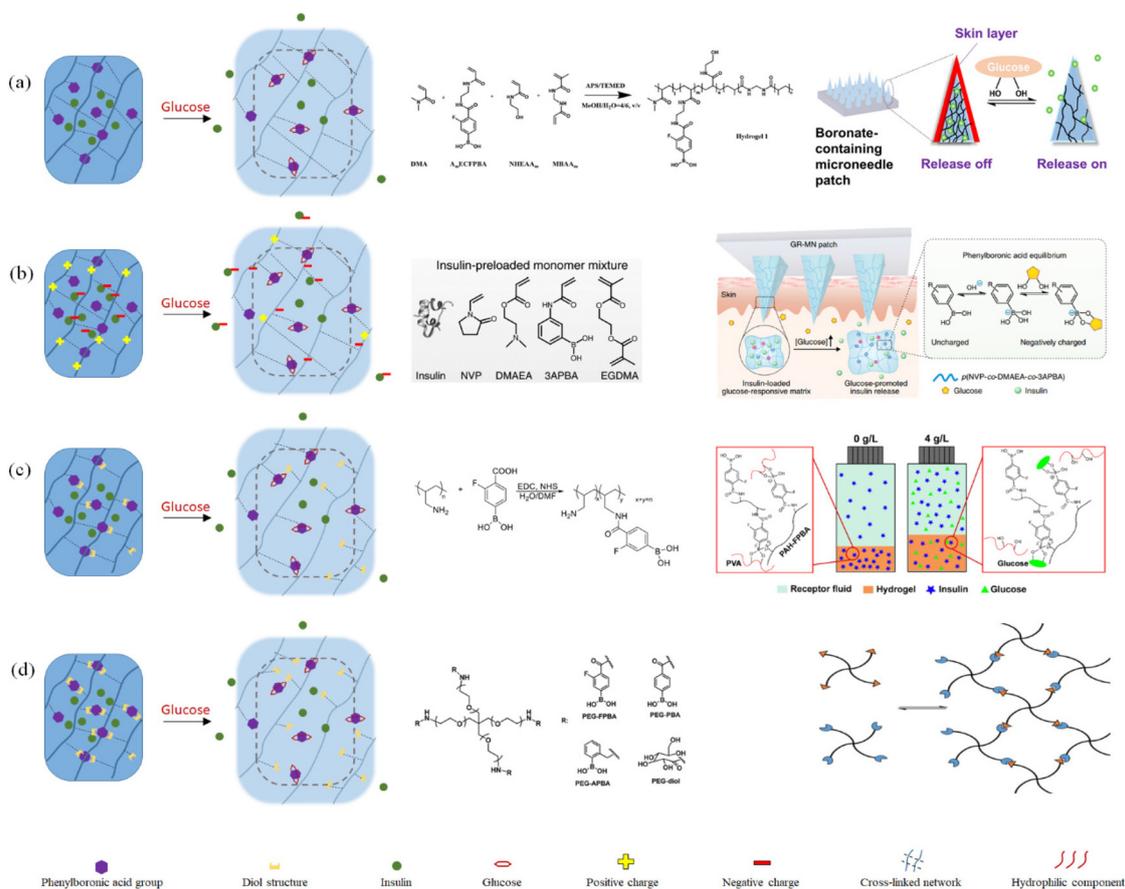

Fig. 16 Schematic diagram of the preparation and release response of phenylboronic acid-based glucose sensitive gels: (a) swollen gel based on hydrophilic–hydrophobic transition. (Adapted with permission from ref. 143. Copyright © 2020, the American Chemical Society.) (b) Swollen gel based on charge transition. (Adapted with permission from ref. 141. Copyright © 2020, The Author(s), under exclusive licence to Springer Nature Limited.) (c) Competition-based polymer-substituted swollen and dissolving gels. (Adapted with permission from ref. 91. Copyright © 2021, the American Chemical Society.) (d) Dissolving gels based on phenylboronic acid as a crosslinker. (Adapted with permission from ref. 145. Copyright © 2015, WILEY-VCH Verlag GmbH & Co. KGaA, Weinheim.).

istics after being combined with glucose, which can weaken the positive electric density in the polymer segment, and thus the electrostatic effect and the swelling of the gel lead to the release of the drug. Xiang Chen *et al.*[91] prepared a polymer segment with polyallylamine as the main chain and grafted it with phenylboronic acid groups. It was mixed with polyvinyl alcohol solution, cross-linked into a hydrogel, and prepared into a microneedle. In a high-glucose environment, the glucose molecules could replace the diols on phenylboronic acid and polyvinyl alcohol to form a more strongly bound borate ester bond, and thus the gel swells with partial dissolution (Fig. 16(c)). Daniel G. Anderson *et al.*[145] prepared polyethylene glucosel macromonomers containing phenylboronic acid groups and diols, and the macromonomers could act as cross-linking agents and form a cross-linked network with each other. When a glucose molecule was specifically bound to the phenylboronic acid group, the gel network dissociated to a greater extent, thus releasing the drug (Fig. 16(d)).

The four gel-based glucose-sensitive models can achieve drug loading and timely glucose-sensitive response. However, the dissolving gel has a quicker glucose sensitive response, while the swollen gel has a slower release. Greater cyclic release can be achieved by the gel using the hydrophilic–hydrophobic transition as the release principle. In addition, more drugs can be carried by gels that use charge transition as their release principle.

4.3.2. Preparation and glucose regulation of glucose-responsive nanoparticle models. Di Shen *et al.*[140] prepared amorphous nanoparticles by altering the phenylboronic acid groups on polylysine segments (Fig. 17(a)). The positively

charged amino groups on lysine have the potential to interact electrostatically with insulin, which is advantageous for drug loading. The hydrophilicity of the segment changed when the glucose molecule was combined with the phenylboronic acid group on the polymer segment. Consequently, the particle structure tended to be looser and the drug was released. Linqi Shi *et al.*[146] synthesized block copolymers containing phenylboronic acid groups and ethylene glucosel, and block copolymers containing AA and glucosyl units, AGA (Fig. 17(b)). The phenylboronic acid group in the two types of polymer segments could interact with the glucosyl unit, AGA, and assembled into a denser micelle structure in solution. When the glucose molecule appeared, it replaced AGA and interacted with the phenylboronic acid group. At this point, the internal density of the particles changed, the internal hydrophilicity was greatly improved, the particle structure was destroyed and the drug was released. As shown in Fig. 17(c), Zaizai Tong *et al.*[147] prepared a polymer segment containing a phenylboronic acid group and a phenylboronic acid pinacol ester group by RAFT polymerization. More hydrophobic phenylboronic acid and phenylboronic acid pinacol ester components were filled inside the particle, whereas the PEG component was dispersed outside the particle due to its hydrophilic properties. Subsequently, insulin and glucose oxidase were loaded in the particles. When glucose molecules entered the particles, glucose oxidase broke down the glucose to create gluconic acid and hydrogen peroxide, and then the hydrogen peroxide broke down the phenylboronic acid pinacol ester. Phenylboronic acid also formed a bond with glucose to cause the corresponding changes. Consequently, the drug was released.
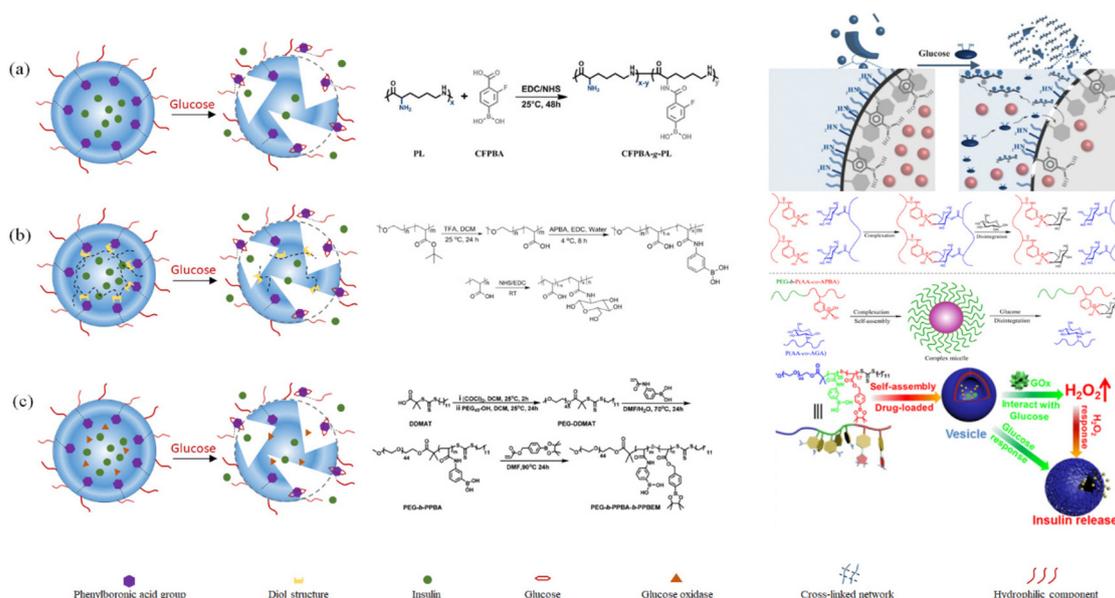

Fig. 17 Schematic diagram of the preparation and release response of phenylboronic acid-based glucose-sensitive nanoparticles: (a) dissociated particles based on hydrophilic–hydrophobic transition, (Adapted with permission from ref. 140. Copyright © 2015, The Royal Society of Chemistry.) (b) Dissociated particles based on competitive substitution. (Adapted with permission from ref. 146. Copyright © 2012, the American Chemical Society.) (c) Dissociative particles combined with glucose oxidase and phenylboronic acid groups. (Adapted with permission from ref. 147. Copyright © 2018, the American Chemical Society.).

All three types of glucose-sensitive model based on nanoparticles respond to glucose relatively quickly. Due to their straightforward structure, the first type of nanoparticles can release the drug the most quickly. The second type of particles had a denser internal structure and perhaps a longer release time because they underwent a competitive substitution in the glucose-sensitive response. The third type of particle contains two types of glucose sensitive responses, *i.e.*, glucose oxidase and phenylboronic acid groups. These groups have a faster glucose-sensitive response rate, but they may also affect the effective drug loading.

4.3.3. Preparation and glucose regulation of other glucose-responsive composite models.

There are numerous complex structures and multi-material combinations of glucose-sensitive models in addition to gel and nanoparticle versions. Xiangdong Kong et al.[148] modified the polymer segment of phenylboronic acid groups grafted on the surface of silica to prepare Met@HMSNs-PAPBA glucose-sensitive microspheres

(Fig. 18(a)). The polymer on the surface was induced by glucose. The segments became more hydrophilic, thereby releasing the drug. Hossein Baharvand et al.[151] developed a microneedle body structure based on porous silica and macroporous alumina, and the chitosan gel covered the surface of the pores, enabling the loading of drugs (Fig. 18(b)). Glucose oxidase was added as a glucose-sensitive factor, and glucose oxidase converted glucose into gluconic acid, which promoted the swelling of the chitosan gel to release the drug.

Yu Tang et al.[149] prepared insulin-containing metal–organic frameworks containing glucose oxidase and silica particles containing Zn^{2+} and Co^{2+} ions (Fig. 18(c)). Glucose oxidase converted glucose into gluconic acid and hydrogen peroxide, and the local acidic environment promoted the dissociation of the metal organic framework to release the drug. Also, Zn^{2+} and Co^{2+} could combine the by-product hydrogen peroxide and decompose it. Zaizai Tong et al.[150] prepared a vesicular glucose-sensitive model formed by self-assembly with pillar 5
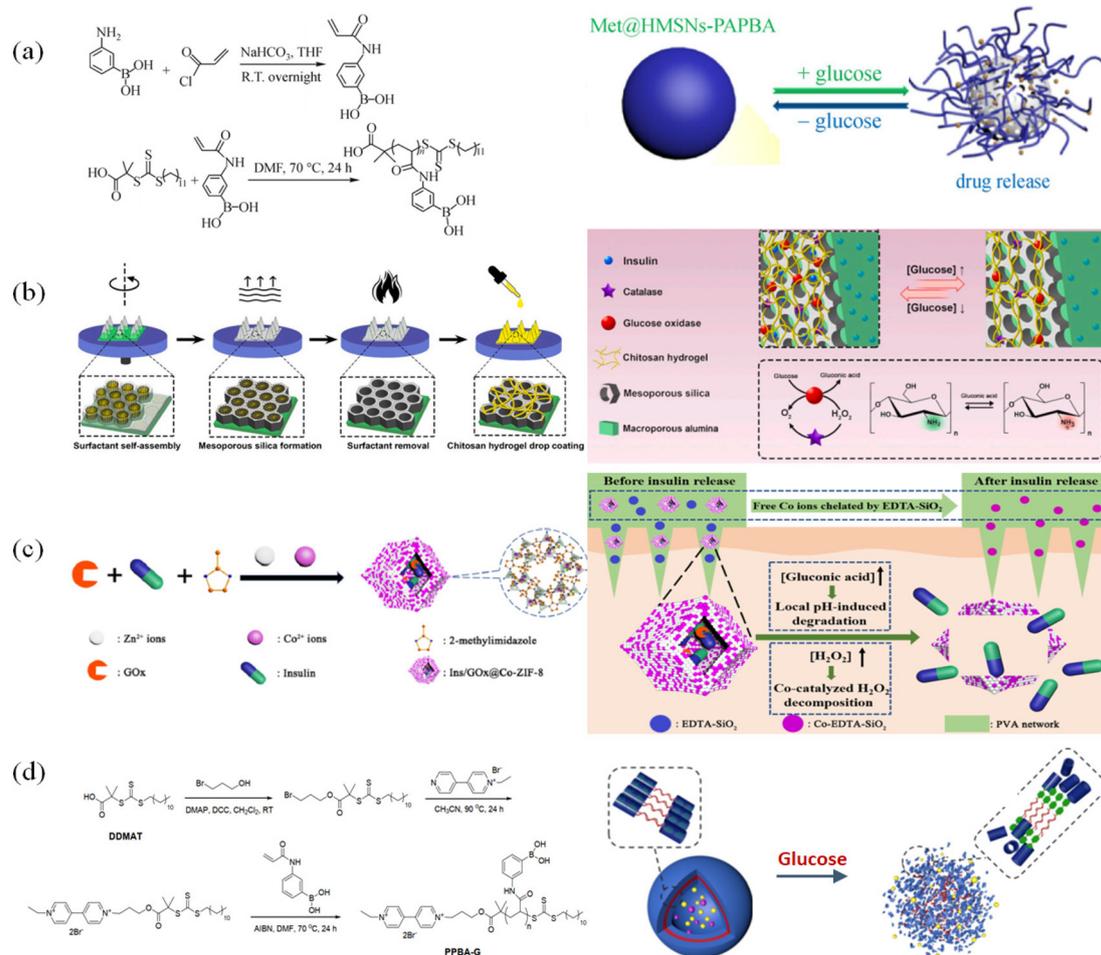

Fig. 18 Composite structure polymer-based glucose-sensitive model. (a) Polymer-grafted hollow mesoporous silica nanoparticles. (Adapted with permission from ref. 148. Copyright © 2021, Higher Education Press.) (b) Dynamically capped hierarchically porous structure. (Adapted with permission from ref. [151] © 2020, Elsevier B.V. All rights reserved.) (c) Mimic multi-enzyme metal–organic framework structure. (Adapted with permission from ref. 149. Copyright © 2020, the American Chemical Society.) (d) Glucose and pH-responsive supramolecular polymer vesicles based on host–guest interaction. (Adapted with permission from ref. 150. Copyright © 2020, the American Chemical Society.).

arene as the external hydrophilic host structure and guest structure composed of paraquat and phenylboronic acid groups, as shown in Fig. 18(d). The glucose-sensitive models contained insulin and glucose oxidase inside. Similarly, under the action of glucose oxidase, gluconic acid was produced. In an acidic environment, the amino group on the host structure would be protonated, and thus the host–guest structure was destroyed, thereby releasing insulin.

These four different types of complex glucose-sensitive models are made up of both organic and inorganic components, and their diverse frameworks and structures give them sensitive release mechanisms. Drug carriers made of inorganic substances such as silica, alumina, and sodium bicarbonate can increase the loading effectiveness. A longer release time can be achieved by designing materials with porous or multiple layers. However, glucose oxidase is typically used in conjunction with inorganic materials. After-treatment residue and by-products such as gluconic acid and hydrogen peroxide can result in immune rejection and other adverse reactions.

4.3.4. Comparison of hydrogel and nanoparticle glucose-sensitive models. The response mechanism of phenylboronic acid-based glucose sensitive gels are mostly based on the specific binding of phenylboronic acid groups to glucose molecules. The response mechanism of phenylboronic acid-based nanoparticles is often dominated by the transition of hydrophilicity and hydrophobicity in the segment structure. A glucose-sensitive model using charge as the response mechanism was reported. The phenylboronic acid group can function in the gel structure as a branch in the molecular segment or as a point of cross-linking in the network to form a stable interpenetrating network structure to load and deliver drugs

(Fig. 19(a)). The phenylboronic acid group is frequently enclosed as a hydrophobic component inside the nanoparticle structure (Fig. 19(b)), and the exterior of the particle is a hydrophilic structure. When glucose molecules pass through the particle gap, the phenylboronic acid groups combine with glucose to enhance their binding ability with water. Consequently, the interior of the particle, which is initially more hydrophobic, changes from hydrophobic to hydrophilic. Therefore, the structural integrity of the nanoparticles is compromised, completing the drug release.

Compared with the nanoparticle-based glucose sensitive model, the gel-based glucose sensitive model can carry more loaded drugs. Also, in the glucose-sensitive response release link, a more obvious drug sustained-release effect can be realized, which is more effective to avoid excessive treatment. The nanoparticle-based glucose sensitive model can reduce the loss of the drug during transport and the drug mixed inside the particle does not easily diffuse, improving the drug utilization rate. It has more sensitive recognition and response to the blood glucose concentration with a smaller volume of nanoparticles. However, these two models have common problems in the experiment of simulating the complex change of normal human blood glucose. Firstly, when the blood glucose concentration occurs in a large area and regularly and repeatedly rises and falls, the existing glucose-sensitive model has insufficient coping ability. The glucose-response effect of the glucose-sensitive model includes the recognition rate of blood glucose and the release rate of the drug. After the first glucose-sensitive release is completed, the effect of each subsequent time is lower than the previous one. Secondly, after each release of the drug treatment, when the blood glucose returns
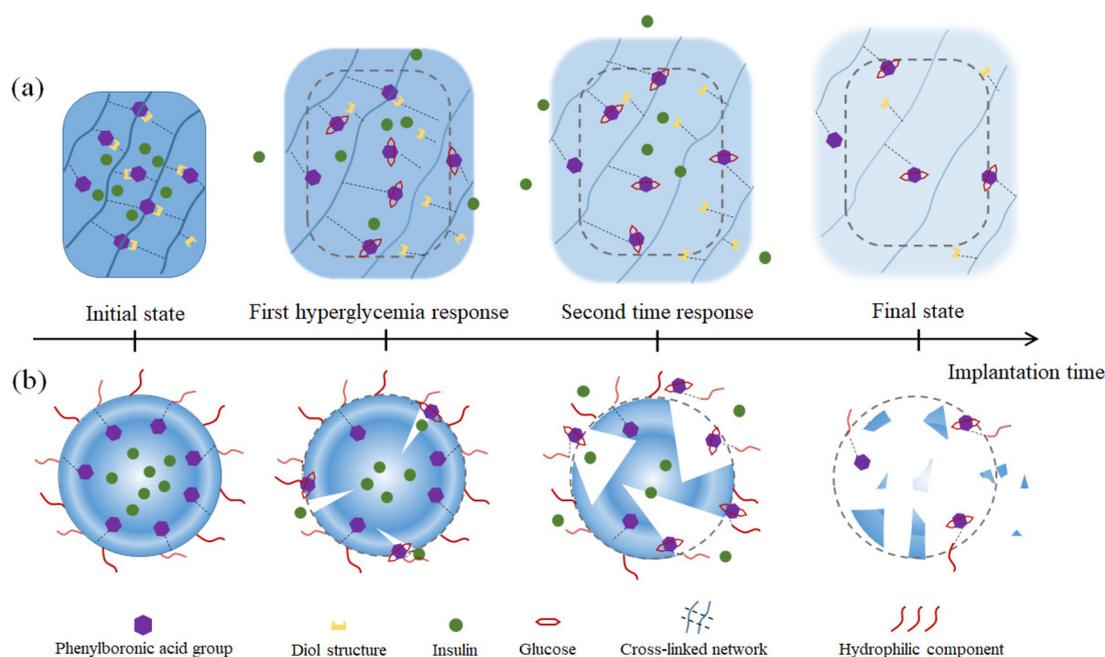

Fig. 19 Initial state, repeated response and final state of phenylboronic-based polymer glucose-sensitive model implanted in the human body. (a) Gel-phenylboronic acid-based glucose-sensitive model. (b) Nanoparticle-phenylboronic acid-based glucose sensitive model.

to the normal range, it is also an urgent problem to effectively control the excessive release of the drug to avoid the risk of hypoglycemia and reduce the ineffective use of the drug.

To meet the precise treatment requirements of various diabetic patients, it is necessary to choose reasonable materials, prepare a matching model size, and use a variety of glucose-sensitive mechanisms that complement each another.

5. Therapeutic effect and evaluation of GSMSs

Thus far, GSMSs have shown significant advantages in the field of diabetes treatment after nearly ten years of development. However, GSMSs still need to undergo a certain degree of testing before clinical trials. By analyzing the existing research results, we found that the safety, hypoglycemic effect, and patient acceptance of GSMSs can be used as a measure to comprehensively summarize the therapeutic effect of microneedles (Fig. 20). (1) Hypoglycemic effect: it is necessary to consider the initial hypoglycemic rate, which is closely associated with the risk of hypoglycemia. In addition, the effective duration of blood glucose control and the minimum blood glucose value represent the long-term therapeutic potential and therapeutic safety indicators of GSMS, respectively. (2) MN material safety: this is a key factor in the success of GSMSs through clinical trials. The glucose-responsive substances in the microneedles and the other main materials determine the safety factor of microneedle therapy. Therefore, the selected glucose-responsive substances and auxiliary materials should have good biocompatibility, and their biosafety such as cytotoxicity, blood compatibility and histocompatibility should be strictly examined. (3) Treatment acceptance: one of the original

goals of GSMSs was to improve the significant pain and skin damage associated with subcutaneous injection therapy. Therefore, the pain, convenience and frequency of GSMS treatment need to be carefully investigated. Similarly, the test results of these three items are also the most important factors to measure before clinical use. Based on the controlled drug release and therapeutic effect of GSMSs, an evaluation method for the therapeutic effect of GSMSs can be established, which can be used to identify and determine the feasibility and therapeutic effectiveness of GSMSs.

5.1. Safety of microneedle materials, hypoglycemic effect of glucose-sensitive models and treatment acceptance of patients

The safety of GSMSs is illustrated by the characterization of the biocompatibility of the materials used. The microneedles need to directly penetrate the epidermis of the skin and enter the human body. Therefore, factors such as cytotoxicity, tissue safety, and blood compatibility of the materials used in microneedles are crucial. The type of microneedle can be used to determine the treatment for which the microneedle stays in the skin. It is also necessary to conduct a comprehensive exploration of its potential rejection reaction in advance.

The patient acceptance of GSMSs, patient compliance and the degree of mental loss after long-term treatment depend on the pain of microneedle treatment. Moreover, the pain level is determined by the size and morphology of the microneedles. Studies have shown that when the length of the microneedles is in the range of 500 to 1200 μm, the puncture treatment will not cause obvious pain.

The hypoglycemic effect of GSMSs is the most important and intuitive criterion for their use as a treatment strategy for diabetes. The hypoglycemic rate and effective hypoglycemic range can measure the therapeutic effect of GSMSs. The "skin-layer" structural glucose-sensitive model proposed by Akira Matsumoto *et al.* could accurately identify changes in glucose concentration and rapidly adjust the drug release rate accordingly (Fig. 21(a) and (b)).[152] The rate and extent of glucose sensitivity of this system could be characterized by *in vitro* release testing. The response to different glucose concentrations also reflected the range and degree of drug release control by the GSMS. The hydrogel–micelle composite glucose-sensitive model established by Linqi Shi *et al.* had different release capacities under various glucose concentrations, and also showed repeatable alternate release performance in environments with different glucose concentrations (Fig. 21(d) and (e)).[153]

The ability of the GSMS to actually treat diabetes was characterized by release tests in live mice, rabbits, pigs and other animals. Meanwhile, the drug release test *in vivo* was also closer to the actual clinical application. Zhen Gu *et al.* showed that the GSMS could make the drug stay in the mouse for the longest time compared with other treatments, and intelligently regulated the insulin release according to the blood glucose concentration (Fig. 22).[53] The actual effect of the GSMS could be investigated in a complex *in vivo* environment. Differentiated research on individual conditions is conducive
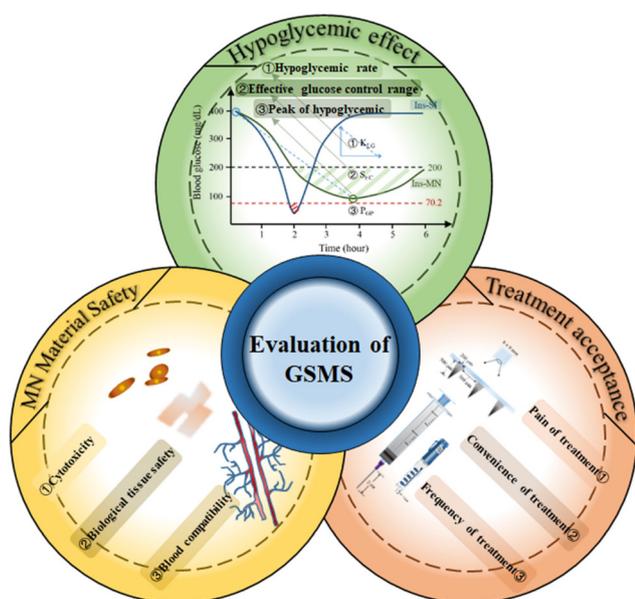

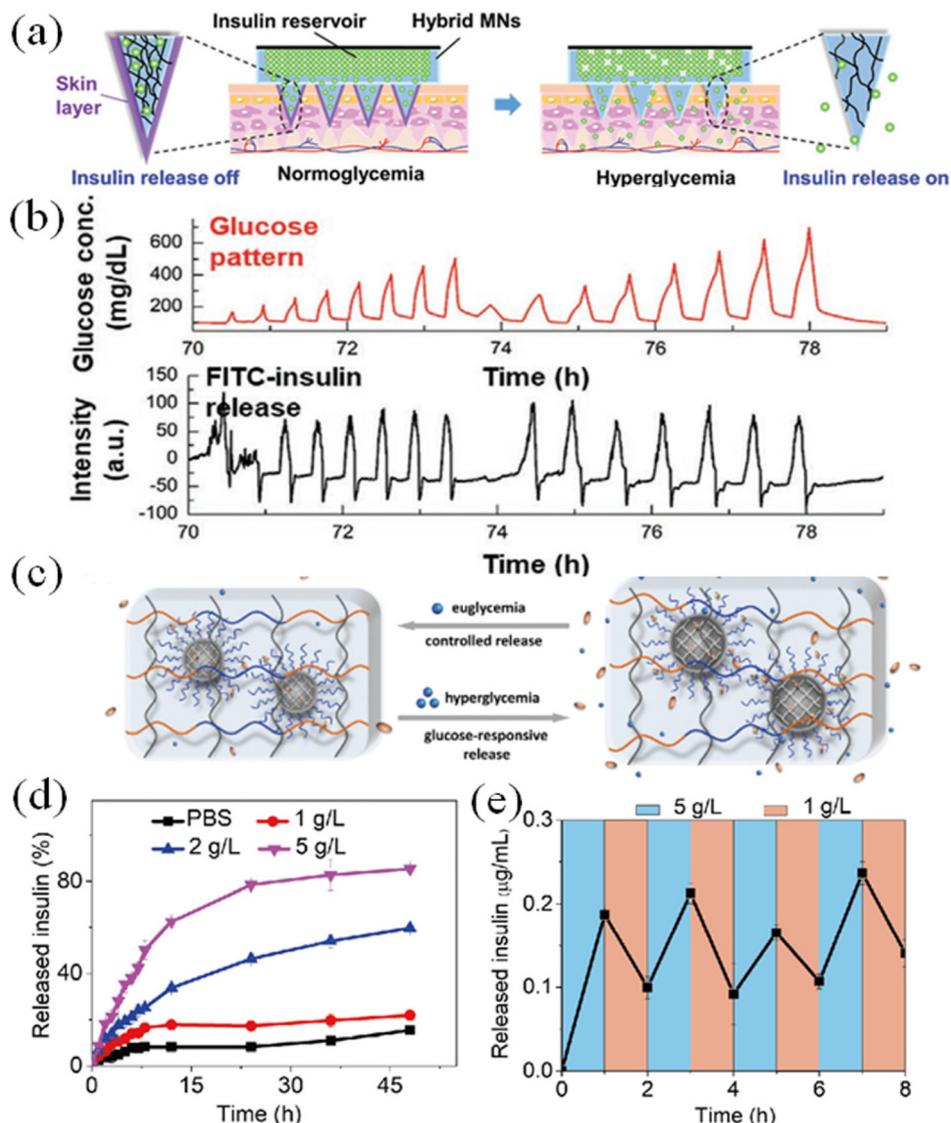**Fig. 20** Evaluation of the therapeutic effect of GSMSs.

Fig. 21 (a) "Skin-layer"-controlled glucose-responsive insulin release from MN-array patch. (b) Day 3 snapshot from the long-term *in vitro* insulin release experiment using reservoir-attached MNs. (Adapted with permission from ref. 152. Copyright © 2021, Wiley-VCH GmbH.) (c) Schematic of reversible insulin release from hydrogel-micelle composite. (d) *In vitro* accumulated insulin released from hydrogel-micelles composite. (e) Pulsatile release profile of hydrogel-micelle composite carrier presents the rate of insulin release as a function of glucose concentration. (Adapted with permission from ref. 153. Copyright © 2019, Science China Press and Springer-Verlag GmbH Germany, part of Springer Nature.).

to the development of various types of GSMS that are applied to different disease scenarios and needs.

5.2. The therapeutic features of glucose-sensitive microneedles compared with traditional subcutaneous injection and sustained-release microneedles

GSMSs are considered to be the best alternative to percutaneous administration such as subcutaneous injection because they can greatly improve the patient treatment compliance. However, there are some controversies and doubts about the drug delivery efficiency and therapeutic effect of GSMSs, as well as the feasibility and stability of the treatment. The most significant point is that compared to subcutaneous insulin

injection (set at 100% drug utilization), the drug utilization rate of GSMSs is relatively low. Part of the drug will remain in the microneedle patch, leading to drug waste. This problem can be avoided by designing the internal space structure of the microneedle and improving the method of the microneedle, such as designing a layered structure, pore structure and multiple injection molding methods to control the distribution of the drug in the microneedle. Consequently, the drug will be fully distributed on the tip of the microneedle, avoiding waste in the patch part and improving the drug utilization rate of the GSMS.

For a sustained-release microneedle system (without glucose-sensitive models) and GSMSs, given that the drug is
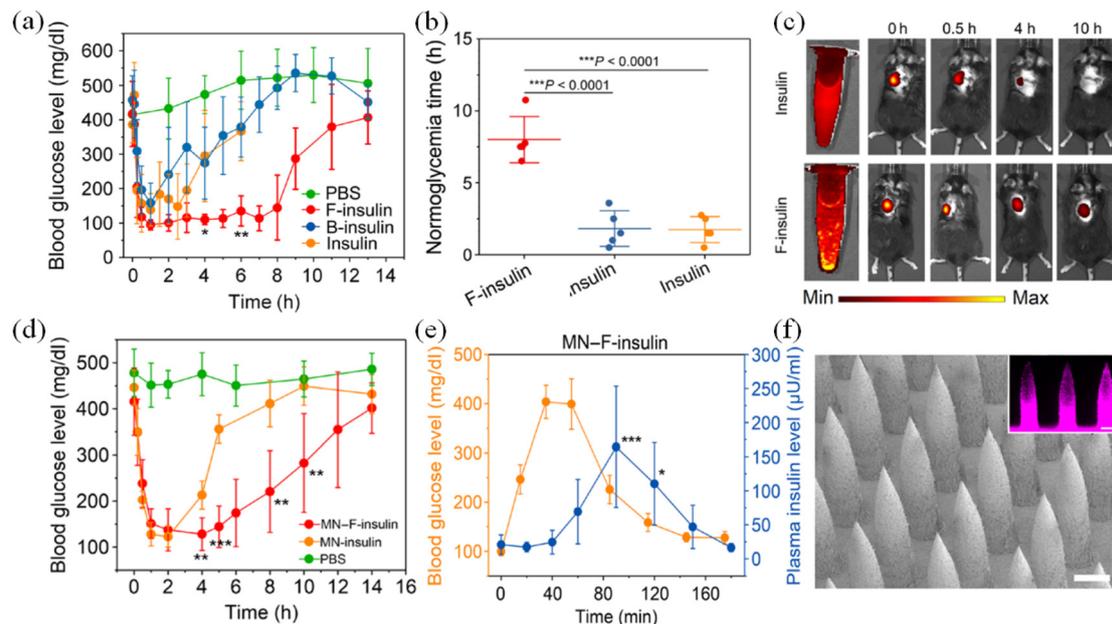
Fig. 22 *In vivo* evaluation of insulin complex for treatment of type 1 diabetic mice. (a) BGLs of type 1 diabetic mice treated with subcutaneously injected native insulin, F-insulin, or B-insulin. PBS was used as a control. The insulin-equivalent dose was 80 U kg^{-1}. (b) Normoglycemic time. (c) Live imaging of subcutaneously injected F-insulin and native insulin labeled with sulfo-Cy5. (d) BGLs of type 1 diabetic mice treated with MN array patches loaded with insulin (MN-insulin) or F-insulin (MN–F-insulin) (2 mg of insulin per patch). Blank MN loaded with PBS was used as a negative control. (e) *In vivo* glucose responsive insulin release triggered by intraperitoneal glucose injection at 3 h after treatment of MN array patch load with F-insulin. (f) Representative scanning electron microscopy image of the MN arrays. (Adapted with permission from ref. 53. Copyright © 2021, American Pharmacists Association. Published by Elsevier Inc. All rights reserved.).

encapsulated inside the microneedles, it needs to go through the swelling or dissolution of the microneedle shell before it can be released. Therefore, both glucose-sensitive microneedles and sustained-release microneedles show similar slow drug release. The findings by Zhen Gu *et al.* provided strong data supporting this view. Sustained-release microneedles and glucose-sensitive microneedles had a longer-lasting release, and the release rate depended on the material and structure of the microneedles. Moreover, the plasma insulin concentration was also avoided, preventing the risk of overtreatment (Fig. 23(b), (c) and (h)).[141] Differently, compared with subcutaneous injection, which can lead to a sudden drop in blood glucose and excessive drug release, GSMSs reflect a safer blood glucose change trend and treatment.

Meanwhile, compared with GSMSs, the drug release law of sustained-release microneedles is also a one-way acceleration, which reflects the characteristics of controllable release in the early stage but uncontrollable in the later stage (it is not affected by changes in the blood glucose concentration). Sustained-release microneedles simply reduce the rate of drug release and increase the length of time that the drug is released. GSMSs can adjust the release rate of the drug in real time according to the change in the blood glucose concentration. The drug release rate and the blood glucose concentration show a positive correlation change law. In the glucose tolerance test, as shown in Fig. 23(e), (f) and (i), it could be seen that the drug release by the GSMS was affected by the

blood glucose concentration. The GSMS could not only prolong the release time of the drug but also avoided the harm caused by the sudden release and excessive release of the drug to the greatest extent, and it was closer to the normal insulin secretion and blood glucose control law by the body. As a more intelligent and effective treatment method, GSMSs have gradually shown great advantages.

5.3. Pharmacological availability, relative bioavailability, and controlled drug release effect of GSMS

The therapeutic effect of GSMSs can be judged more intuitively compared with subcutaneous insulin injection. In the blood glucose concentration curve during the delivery of insulin drug therapy, several factors should be considered including the rate of hypoglycemia, the peak and corresponding time of hypoglycemia, and the area of effective hypoglycemia. Correspondingly, in the blood insulin concentration curve, it is necessary to pay special attention to the insulin rise rate, insulin peak value and corresponding time, and insulin-safe concentration treatment area. Meanwhile, the glucose tolerance test was used to illustrate the glucose response performance of the GSMS. The time interval between the peak point of blood glucose and the peak point of insulin was the response time of the glucose-sensitive model. In repeated blood glucose change tests, the stability, blood glucose dependence, and release controllability of the glucose-sensitive model can be detected. According to Formulas (1) and (2), the pharmacological availability (PBA) and relative bio-
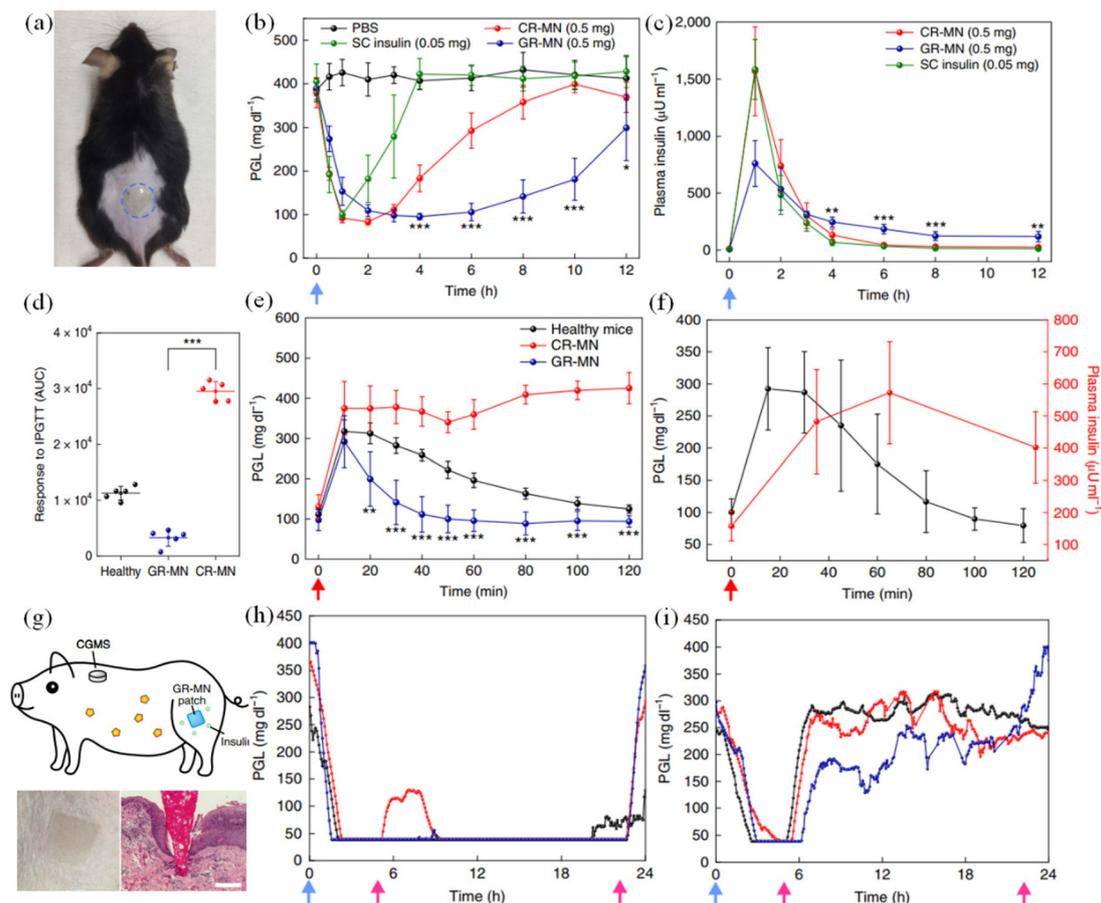
Fig. 23 *In vivo* evaluation of the GR-MN patch in an STZ-induced diabetic mouse and minipig model. (a) Mouse dorsum skin (the area within the blue dashed line) transcutaneously treated with a microneedle patch. (b) and (c) Blood glucose level treated with microneedle patch. (d) Responsiveness in diabetic mice was calculated based on the area under the curve (AUC) from 0–120 min, with the baseline set at the 0 min plasma glucose reading. (e) *In vivo* intraperitoneal glucose tolerance test in diabetic mice. (f) *In vivo* glucose responsive insulin release promoted by intra-peritoneal glucose challenge at 4 h post-administration of GR-MN in diabetic mice. (g) Schematic of a minipig treated with GR-MN at the leg site and monitored with a CGMS. (h) and (i) Blood glucose level treated with microneedle patch. (Adapted with permission from ref. 141. Copyright © 2020, The Authors, some rights reserved, exclusive licensee American Association for the Advancement of Science.).

availability (RBA) of GSMSs can be quantitatively measured, which are the most commonly used measures at present. If the effective therapeutic effect is defined according to the strict blood glucose level, the range of AUC needs to be limited to 70.2–200 mg dL^{-1} in Formula (1), which can more accurately represent the range of blood glucose recovery brought by the treatment. Here, AAC_{MN} indicates the area above the curve after the application of the insulin-loaded MN patch and AAC_{SI} shows the area above the curve after the intraperitoneal injection of insulin. AUC_{MN} represents the area under the serum concentration-time curve after the administration of the insulin-loaded MN, and AUC_{SI} represents the area under the plasma concentration-time curve after the insulin injection.

$$PBA\ (\%) = (AAC_{MN} \times Dose_{SI})/(AAC_{SI} \times Dose_{MN}) \times 100 \quad (1)$$

$$PBA\ (\%) = (AUC_{MN} \times Dose_{SI})/(AUC_{SI} \times Dose_{MN}) \times 100 \quad (2)$$

However, in many studies, it was found that the actual hypo-glycemic effect of many GSMSs did not reach normal blood glucose levels. This may be due to the fact that the proportion of glucose-sensitive models was not high enough, resulting in poor sensitivity of the glucose-sensitive model. At high glucose concentrations, sufficient insulin cannot be released on demand. Therefore, it is crucial to establish a well-balanced GSMS. The release effect of the GSMS (K_{MN}) is determined by the release efficiency formed by the microneedle structure and material (K_{MS}) and the release efficiency of the glucose-sensitive model (K_{GS}) in the microneedle (Fig. 24). In a high glucose environment, when $K_{GS} > K_{MS}$, the release mode of the glucose-sensitive model dominates. At this time, $K_{MN} = K_{GS}$, and the drug can be released on demand according to the change in blood glucose concentration. In the environment of normal blood glucose and hypogly-cemia, when $K_{GS} < K_{MS}$, the sustained-release performance of the microneedle structure dominates. Here, $K_{MN} = K_{MS}$, which greatly reduces the rate and degree of drug release, and avoids hypoglyce-mia caused by excessive treatment. The GSMS simulates the working state of the normal pancreas in a more efficient and safe way to complete real-time blood glucose regulation.
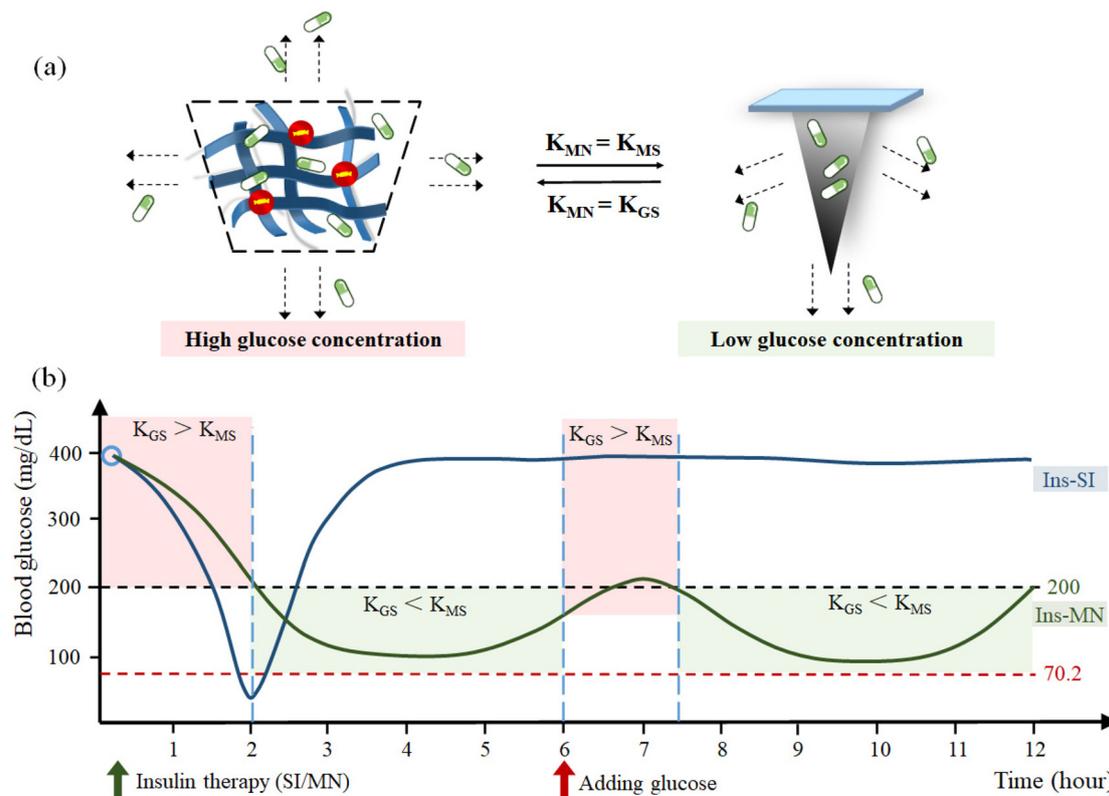
Fig. 24 (a) Influencing factors of KMS at different glucose concentrations. (b) Simulation curve of blood glucose change and drug controlled release.

6.   Summary and outlook

Presently, patients with type 1 diabetes and advanced type 2 diabetes can only be treated by insulin injection. However, there are two main problems associated with subcutaneous injection therapy, *i.e.*, the pain caused by routine injection and the damage of skin tissue caused by repeated treatment. Moreover, if the dosage of hypoglycemic drugs cannot be precisely controlled, it is easy to cause hypoglycemia caused by over treatment, which may be fatal. Alternatively, therapeutic GSMSs can solve the treatment disadvantages caused by subcutaneous injection. There are several challenges to consider before GSMSs can be put into practice, as follows: (1) the different treatment needs and model design of the GSMS and the selection of glucose control strategies and drug delivery models for the corresponding types of hyperglycemias. (2) Preparation and transportation costs of GSMSs and consideration of their preservation environment. Especially the influence of temperature and humidity on the puncture effect and drug activity of microneedles. (3) Characterization of the safety of exogenous materials used in GSMSs. In addition to improving patient compliance, the therapeutic damage to biological tissues, cells and blood can be improved to the greatest extent.

The micron-sized needle body of polymer GSMSs prevents damage to dense neural networks and vascular tissues when penetrating the skin. In addition, the specific recognition of glucose concentration by the glucose-sensitive model can control insulin release more accurately. Currently, polymer GSMSs are associated with some issues, which require optimization and improvement. For instance, when preparing the microneedle, it is vital to increase the production effectiveness, guaranteeing the microneedle yield, while the microneedle should have certain mechanical strength, improved biocompatibility, and anti-inflammatory effect, encouraging additional features such as wound healing. It is necessary to consider the age, disease characteristics, and personal preferences of diabetic patients when choosing glucose control medications. Thus far, GSMS-based studies have progressed from mice and rats to larger mini pigs, bringing them closer to human applications. In addition, related clinical trials are also being actively prepared and carried out. It is certain that GSMSs have shown effective therapeutic effects and significant therapeutic advantages in blood glucose control, and the safety evaluation system for GSMS is becoming more and more comprehensive and perfect. Although there are still some problems to be solved, such as the drug utilization rate of GSMSs, long-term treatment time, monitoring of drug release and other aspects to be further improved, the results achieved have given great confidence and motivation to continue further research.

The drug and microneedle materials must work well together given that the microneedle system is the most essen-

tial component for the glucose-sensitive factor to function properly. Additionally, it can quickly determine the blood glucose level and release the medication as needed in response to variations and changes in the blood glucose levels. Synchronizing the blood glucose regulation based on the variations in blood glucose. The size advantage of therapeutic GSMSs in terms of structure and intelligent, controllable adjustment of glucose-sensitive models can significantly increase patient compliance, improve the drug utilization, and lower the risk of overtreatment. Thus, the research on the microneedle system in the glucose-sensitive model has gradually advanced, making it more effective and intelligent. Finally, GSMSs have great potential as a substitute for the damaged pancreas of the human body to intelligently regulate the blood glucose and achieve the long-term effective treatment of diabetes. As the research progresses, GSMSs may evolve into an optimal diabetes management strategy. Potentially wearable GSMSs can be developed through integration with related technologies such as electronic messaging. Thus, combining the regulation and monitoring of blood glucose with other functions, GSMSs can truly solve the blood glucose disorder and related safety problems plaguing hundreds of millions of diabetic patients.

Conflicts of interest

There are no conflicts to declare.

Acknowledgements

References

1 International Diabetes Federation, Brussels, Belgium, 2021, Available at: https://www.diabetesatlas.org.

2 J. B. Cole and J. C. Florez, *Nat. Rev. Nephrol.*, 2020, **16**, 377–390.

3 J. B. Buse, *J. Am. Med. Assoc.*, 2019, **322**, 1518–1519.

4 E. W. Gregg, I. Hora and S. R. Benoit, *J. Am. Med. Assoc.*, 2019, **321**, 1867–1868.

5 N. Laiteerapong and A. S. Cifu, *J. Am. Med. Assoc.*, 2016, **315**, 697–698.

6 A. T. Hattersley and K. A. Patel, *Diabetologia*, 2017, **60**, 769–777.

7 J. J. Chamberlain, R. R. Kalyani, S. Leal, A. S. Rhinehart, J. H. Shubrook, N. Skolnik and W. H. Herman, *Ann. Intern. Med.*, 2017, **167**, 493–498.

8 G. Rena, D. G. Hardie and E. R. Pearson, *Diabetologia*, 2017, **60**, 1577–1585.

9 S. Sellami, C. Jemaï, S. Chelbi, I. Ksira, N. Ben Amor, R. Ben Mohamed, H. Tartek and F. Ben Mami, *Ann. Endocrinol.*, 2016, **77**, 498–528.

10 K. S. Boye, J. B. Jordan, R. E. Malik, B. M. Currie and L. S. Matza, *Diabetes Ther.*, 2021, **12**, 2387–2403.

11 L. Norton, C. Shannon, A. Gastaldelli and R. A. DeFronzo, *Metabolism*, 2022, **129**, 155142.

12 A. J. Graveling and B. M. Frier, *Diabetes Res. Clin. Pract.*, 2017, **133**, 30–39.

13 A. C. Gonçalves, S. Cavassana, F. R. Chavarette, R. Outa, S. J. Casarin and A. V. Corazza, *J. Healthcare Eng.*, 2020, **1**, 8822686.

14 P. E. Bigeleisen, *Reg. Anesth. Pain Med.*, 2017, **1**, 42–43.

15 L. Nordquist, N. Roxhed, P. Griss and G. Stemme, *Pharm. Res.*, 2007, **24**, 1381–1388.

16 H. S. Gill and M. R. Prausnitz, *J. Diabetes Sci. Technol.*, 2007, **1**, 725–729.

17 Y. Ye, J. Yu, C. Wang, N.-Y. Nguyen, G. M. Walker, J. B. Buse and Z. Gu, *Adv. Mater.*, 2016, **28**, 3115–3121.

18 Y. Zeng, J. Wang, Z. Wang, G. Chen, J. Yu, S. Li, Q. Li, H. Li, D. Wen and Z. Gu, *Nano Today*, 2020, **35**, 100984.

19 J. Gupta, E. I. Felner and M. R. Prausnitz, *Diabetes Technol. Ther.*, 2011, **13**, 451–456.

20 N. Roxhed, B. Samel, L. Nordquist, P. Griss and G. Stemme, *IEEE Trans. Biomed. Eng.*, 2008, **55**, 1063–1071.

21 B. Al-Qallaf and D. B. Das, *Chem. Eng. Sci.*, 2008, **63**, 2523–2535.

22 Y. Wu, Y. Gao, G. Qin, S. Zhang, Y. Qiu, F. Li and B. Xu, *Biomed. Microdevices*, 2010, **12**, 665–671.

23 S. Liu, M.-n. Jin, Y.-s. Quan, F. Kamiyama, H. Katsumi, T. Sakane and A. Yamamoto, *J. Controlled Release*, 2012, **161**, 933–941.

24 K. Ita, *Biomed. Pharmacother.*, 2017, **93**, 1116–1127.

25 I. H. de Boer, S. Bangalore, A. Benetos, A. M. Davis, E. D. Michos, P. Muntner, P. Rossing, S. Zoungas and G. Bakris, *Diabetes Care*, 2017, **40**, 1273–1284.

26 American Diabetes Association Professional Practice Committee, *Diabetes Care*, 2021, **45**, S97–S112.

27 E. J. Sanchez and W. T. Cefalu, *Circulation*, 2019, **140**, 526–528.

28 K. Lian, H. Feng, S. Liu, K. Wang, Q. Liu, L. Deng, G. Wang, Y. Chen and G. Liu, *Biosens. Bioelectron.*, 2022, **203**, 114029.

29 S. Chelbi, K. Ben Naceur, I. Oueslati, N. Bendag, A. Smida, S. Sellami, A. Temessek and F. B. Mami, *Ann. Endocrinol.*, 2018, **79**, 463–501.

30 P. Aschner, *Am. J. Ther.*, 2020, **27**, 79–90.

31 C. J. Rini, E. McVey, D. Sutter, S. Keith, H.-J. Kurth, L. Nosek, C. Kapitza, K. Rebrin, L. Hirsch and R. J. Pettis, *Drug Delivery Transl. Res.*, 2015, **5**, 332–345.

32 F. Bock, E. Lin, C. Larsen, H. Jensen, K. Huus, S. W. Larsen and J. Østergaard, *Eur. J. Pharm. Sci.*, 2020, **145**, 105239.

33 Y. Ito, T. Nakahigashi, N. Yoshimoto, Y. Ueda, N. Hamasaki and K. Takada, *Diabetes Technol. Ther.*, 2012, **14**, 891–899.

34 J. J. Norman, M. R. Brown, N. A. Raviele, M. R. Prausnitz and E. I. Felner, *Pediatr. Diabetes*, 2013, **14**, 459–465.

35 B. Lu, A. GhavamiNejad, J. F. Liu, J. Li, S. Mirzaie, A. Giacca and X. Y. Wu, *ACS Appl. Mater. Interfaces*, 2022, **14**, 20576–20590.

36 Q. Wu, L. Wang, H. Yu, J. Wang and Z. Chen, *Chem. Rev.*, 2011, **111**, 7855–7875.

37 A. Larcher, A. Lebrun, M. Smietana and D. Laurencin, *New J. Chem.*, 2018, **42**, 2815–2823.

38 S. H. Khatami, O. Vakili, N. Ahmadi, E. Soltani Fard, P. Mousavi, B. Khalvati, A. Maleksabet, A. Savardashtaki, M. Taheri-Anganeh and A. Movahedpour, *Biotechnol. Appl. Biochem.*, 2022, **69**, 939–950.

39 F. Liu, S. C. Song, D. Mix, M. Baudyš and S. W. Kim, *Bioconjugate Chem.*, 1997, **8**, 664–672.

40 A. K. Yetisen, N. Jiang, A. Fallahi, Y. Montelongo, G. U. Ruiz-Esparza, A. Tamayol, Y. S. Zhang, I. Mahmood, S.-A. Yang, K. S. Kim, H. Butt, A. Khademhosseini and S.-H. Yun, *Adv. Mater.*, 2017, **29**, 1606380.

41 H. Tsuge, O. Natsuaki and K. Ohashi, *J. Biochem.*, 1975, **78**, 835–843.

42 E. Battistel, G. Lazzarini, F. Manca and G. Rialdi, *Eur. Biophys. J.*, 1985, **13**, 1–9.

43 D. Goodsell, Molecule of the Month: Glucose Oxidase, *RCSB Protein Data Ban*, 2006, **15**, 64–75.

44 C. F. Ainsworth and K. D. Hardman, Structure of Concanavalin A at 2.4-A Resolution, *Biochemistry*, 1972, **11**, 4910–4919.

45 J. Yan, G. Springsteen, S. Deeter and B. Wang, *Tetrahedron*, 2004, **60**, 11205–11209.

46 G. Springsteen and B. Wang, *Tetrahedron*, 2002, **58**, 5291–5300.

47 Y. Y. Ma, H. T. Liu, J. H. Ma and J. H. Gong, *Mater. Sci. Forum*, 2018, **913**, 714–721.

48 M. Van Duin, J. A. Peters, A. P. G. Kieboom and H. van Bekkum, *Tetrahedron*, 1984, **40**, 2901–2911.

49 T. Yang, R. Ji, X.-X. Deng, F.-S. Du and Z.-C. Li, *Soft Matter*, 2014, **10**, 2671–2678.

50 W. Bao, W. Hai, L. Bao, F. Yang, Y. Liu, T. Goda and J. Liu, *Mater. Chem. Front.*, 2021, **5**, 7675–7683.

51 F. L. Kearns, C. Robart, M. T. Kemp, S. L. Vankayala, B. M. Chapin, E. V. Anslyn, H. L. Woodcock and J. D. Larkin, *J. Chem. Inf. Model.*, 2019, **59**, 2150–2158.

52 Y. Liu, Y. Liu, Q. Wang, Y. Han and Y. Tan, *Polymer*, 2020, **202**, 122624.

53 J. Wang, J. Yu, Y. Zhang, X. Zhang, A. R. Kahkoska, G. Chen, Z. Wang, W. Sun, L. Cai, Z. Chen, C. Qian, Q. Shen, A. Khademhosseini, J. B. Buse and Z. Gu, *Sci. Adv.*, 2019, **5**, eaaw4357.

54 D. Lee, K. Choe, Y. Jeong, J. Yoo, S. M. Lee, J.-H. Park, P. Kim and Y.-C. Kim, *RSC Adv.*, 2015, **5**, 14482–14491.

55 X. Chen, H. Yu, L. Wang, D. Shen, B. ul Amin, J. Feng, Q. Zhang and W. Xiong, *ChemNanoMat*, 2021, **7**, 1230–1240.

56 P. Zhang, Q. Ma, D. He, G. Liu, D. Tang, L. Liu and J. Wu, *Eur. Polym. J.*, 2021, **157**, 110648.

57 Y. Fu, P. Liu, M. Chen, T. Jin, H. Wu, M. Hei, C. Wang, Y. Xu, X. Qian and W. Zhu, *J. Colloid Interface Sci.*, 2022, **605**, 582–591.

58 Q. Guo, Z. Wu, X. Zhang, L. Sun and C. Li, *Soft Matter*, 2014, **10**, 911–920.

59 Z. Gu, T. T. Dang, M. Ma, B. C. Tang, H. Cheng, S. Jiang, Y. Dong, Y. Zhang and D. G. Anderson, *ACS Nano*, 2013, **7**, 6758–6766.

60 F. Shi, J. Xu, Z. Hu, C. Ren, Y. Xue, Y. Zhang, J. Li, C. Wang and Z. Yang, *Chin. Chem. Lett.*, 2021, **32**, 3185–3188.

61 M. L. Agazzi, S. E. Herrera, M. L. Cortez, W. A. Marmisollé, M. Tagliazucchi and O. Azzaroni, *Chem. – Eur. J.*, 2020, **26**, 2456–2463.

62 K. Yoshida, K. Awaji, S. Shimizu, M. Iwasaki, Y. Oide, M. Ito, T. Dairaku, T. Ono, Y. Kashiwagi and K. Sato, *Polymers*, 2018, **10**, 44–51.

63 A. van der Vliet and Y. M. W. Janssen-Heininger, *J. Cell. Biochem.*, 2014, **115**, 427–435.

64 J. Pravda, *Mol. Med.*, 2020, **26**, 41–51.

65 J. L. Meitzler, M. M. Konaté and J. H. Doroshow, *Arch. Biochem. Biophys.*, 2019, **675**, 108076.

66 K. Kikuchi-Torii, S. Hayashi, H. Nakamoto and S. Nakamura, *J. Biochem.*, 1982, **92**, 1449–1456.

67 J. Switala and P. C. Loewen, *Arch. Biochem. Biophys.*, 2002, **401**, 145–154.

68 P. Bendinelli, P. Maroni, E. Matteucci and M. A. Desiderio, *Int. J. Mol. Sci.*, 2016, **17**, 706–717.

69 R. C. Augustin, G. M. Delgoffe and Y. G. Najjar, *Cancers*, 2020, **12**, 3802.

70 M. Huelsemann, L. P. Frenzel, D. Baatout, J. Claasen, S. Theurich, L. Kintzelé, H. J. Becker, M. Patz, C. P. Pallasch, M. S. von Bergwelt-Baildon, M. Hallek and C.-M. Wendtner, *Blood*, 2012, **120**, 3918–3918.

71 E. Boedtkjer and S. F. Pedersen, *Annu. Rev. Physiol.*, 2020, **82**, 103–126.

72 Z. Zhang, Q. Lai, Y. Li, C. Xu, X. Tang, J. Ci, S. Sun, B. Xu and Y. Li, *Sci. Rep.*, 2017, **7**, 46161.

73 W.-j. Zhang, *Purinergic Signalling*, 2021, **17**, 151–162.

74 J. J. Kim and K. Park, *Pharm. Res.*, 2001, **18**, 794–799.

75 R. Ballerstadt, C. Evans, R. McNichols and A. Gowda, *Biosens. Bioelectron.*, 2006, **22**, 275–284.

76 C. F. Brewer, H. Sternlicht, D. M. Marcus and A. P. Grollman, *Biochemistry*, 1973, **12**, 4448–4457.

77 T. Ye, S. Yan, Y. Hu, L. Ding and W. Wu, *Polym. Chem.*, 2014, **5**, 186–194.

78 R. Yin, Z. Tong, D. Yang and J. Nie, *Int. J. Biol. Macromol.*, 2011, **49**, 1137–1142.

79 U. Novak and J. Grdadolnik, *J. Mol. Struct.*, 2017, **1135**, 138–143.

80 T. Wang, G. X. Qin, Y. Zhao and Z. W. Sun, *Food Agric. Immunol.*, 2009, **20**, 295–304.

81 R. Chang, M. Li, S. Ge, J. Yang, Q. Sun and L. Xiong, *Ind. Crops Prod.*, 2018, **112**, 98–104.

82 Y. Mizuno, K. Takasawa, T. Hanada, K. Nakamura, K. Yamada, H. Tsubaki, M. Hara, Y. Tashiro, M. Matsuo, T. Ito and T. Hikima, *Biomed. Microdevices*, 2021, **23**, 38.

83 E. Caffarel-Salvador, S. Kim, V. Soares, R. Y. Tian, S. R. Stern, D. Minahan, R. Yona, X. Lu, F. R. Zakaria, J. Collins, J. Wainer, J. Wong, R. McManus, S. Tamang, S. McDonnell, K. Ishida, A. Hayward, X. Liu, F. Hubálek, J. Fels, A. Vegge, M. R. Frederiksen, U. Rahbek, T. Yoshitake, J. Fujimoto, N. Roxhed, R. Langer and G. Traverso, *Sci. Adv.*, 2021, **7**, eabe2620.

84 X. Zhang, G. Chen, X. Fu, Y. Wang and Y. Zhao, *Adv. Mater.*, 2021, **33**, 2104932.

85 X. P. Zhang, B. B. Wang, L. F. Hu, W. M. Fei, Y. Cui and X. D. Guo, *Biochem. Eng. J.*, 2021, **176**, 108157.

86 M. A. L. Teo, C. Shearwood, K. C. Ng, J. Lu and S. Moochhala, *Biomed. Microdevices*, 2005, **7**, 47–52.

87 B. Z. Chen, M. Ashfaq, X. P. Zhang, J. N. Zhang and X. D. Guo, *J. Drug Targeting*, 2018, **26**, 720–729.

88 M. Wu, Y. Zhang, H. Huang, J. Li, H. Liu, Z. Guo, L. Xue, S. Liu and Y. Lei, *Mater. Sci. Eng., C*, 2020, **117**, 111299.

89 M. Zhu, Y. Liu, F. Jiang, J. Cao, S. C. Kundu and S. Lu, *ACS Biomater. Sci. Eng.*, 2020, **6**, 3422–3429.

90 Y. Xie, R. Shao, Y. Lin, C. Wang, Y. Tan, W. Xie and S. Sun, *Pharmaceutics*, 2021, **13**, 827–843.

91 X. Chen, H. Yu, L. Wang, D. Shen, C. Li and W. Zhou, *ACS Biomater. Sci. Eng.*, 2021, **7**, 4870–4882.

92 J. Li, Y. Zhou, J. Yang, R. Ye, J. Gao, L. Ren, B. Liu, L. Liang and L. Jiang, *Mater. Sci. Eng., C*, 2019, **96**, 576–582.

93 Z. Xiang, H. Wang, S. K. Murugappan, S.-C. Yen, G. Pastorin and C. Lee, *J. Micromech. Microeng.*, 2015, **25**, 025013.

94 N. Zhang, X. Zhou, L. Liu, L. Zhao, H. Xie and Z. Yang, *Front. Pharmacol.*, 2021, **12**, 719905.

95 S. Zhu, B. Zhang, Y. Wang, Y. He, G. Qian, L. Deng and Z.-R. Zhang, *J. Drug Delivery Sci. Technol.*, 2021, **62**, 102336.

96 W. J. Liu, W. J. Guo, M. Yang, X. D. Zhang and F. H. Wu, *Polym. Bull.*, 2022, **79**, 867–882.

97 Y. Mizuno, K. Takasawa, T. Hanada, K. Nakamura, K. Yamada, H. Tsubaki, M. Hara, Y. Tashiro, M. Matsuo, T. Ito and T. Hikima, *Biomed. Microdevices*, 2021, **23**, 38–46.

98 X. P. Zhang, B. B. Wang, L. F. Hu, W. M. Fei, Y. Cui and X. D. Guo, *Biochem. Eng. J.*, 2021, **176**, 108157.

99 L. Fan, X. Zhang, X. Liu, B. Sun, L. Li and Y. Zhao, *Adv. Healthcare Mater.*, 2021, **10**, 2002249.

100 R. E. Sully, H. Garelick, E. Z. Loizidou, A. G. Podoleanu and V. Gubala, *Mater. Adv.*, 2021, **2**, 5432–5442.

101 Z. Y. Zeng, G. H. Jiang, T. Q. Liu, G. Song, Y. F. Sun, X. Y. Zhang, Y. T. Jing, M. J. Feng and Y. F. Shi, *Bio-Des. Manuf.*, 2021, **4**, 902–911.

102 T. Q. Liu, G. H. Jiang, G. Song, Y. F. Sun, X. Y. Zhang and Z. Y. Zeng, *J. Pharm. Sci.*, 2021, **110**, 3004–3010.

103 Y. P. Wang, S. Y. Cheng, W. Hu, X. Lin, C. Cao, S. F. Zou, Z. Z. Tong, G. H. Jiang and X. D. Kong, *Front. Mater. Sci.*, 2021, **15**, 98–112.

104 M. M. Zhu, Y. Liu, F. J. Jiang, J. X. Cao, S. C. Kundu and S. Z. Lu, *ACS Biomater. Sci. Eng.*, 2020, **6**, 3422–3429.

105 A. Ullah, H. J. Choi, M. Jang, S. An and G. M. Kim, *Pharmaceutics*, 2020, **12**, 606–620.

106 Y. H. Lin, W. Hu, X. W. Bai, Y. S. Ju, C. Cao, S. F. Zou, Z. Z. Tong, C. Cen, G. H. Jiang and X. D. Kong, *ACS Appl. Bio Mater.*, 2020, **3**, 6376–6383.

107 D. F. S. Fonseca, P. C. Costa, I. F. Almeida, P. Dias-Pereira, I. Correia-Sa, V. Bastos, H. Oliveira, M. Duarte-Araujo, M. Morato, C. Vilela, A. J. D. Silvestre and C. S. R. Freire, *Carbohydr. Polym.*, 2020, **241**, 116314.

108 L. K. Vora, A. J. Courtenay, I. A. Tekko, E. Larraneta and R. F. Donnelly, *Int. J. Biol. Macromol.*, 2020, **146**, 290–298.

109 M. X. Wu, Y. J. Zhang, H. Huang, J. W. Li, H. Y. Liu, Z. Y. Guo, L. J. Xue, S. Liu and Y. F. Lei, *Mater. Sci. Eng., C*, 2020, **117**, 36–45.

110 S. Y. Wang, M. M. Zhu, L. Zhao, D. J. Kuang, S. C. Kundu and S. Z. Lu, *ACS Biomater. Sci. Eng.*, 2019, **5**, 1887–1894.

111 Y.-C. Chen, C.-Y. Tsai, C.-Y. Lee and I. N. Lin, *Acta Biomater.*, 2014, **10**, 2187–2199.

112 S. Kim, H. Yang, J. Eum, Y. Ma, S. F. Lahiji and H. Jung, *Biomaterials*, 2020, **232**, 119733.

113 Q. Zhang, C. Xu, S. Lin, H. Zhou, G. Yao, H. Liu, L. Wang, X. Pan, G. Quan and C. Wu, *Acta Pharm. Sin. B*, 2018, **8**, 449–457.

114 X. Ning, C. Wiraja, D. C. S. Lio and C. Xu, *Adv. Healthcare Mater.*, 2020, **9**, 2000147.

115 J.-T. Choi, S.-J. Park and J.-H. Park, *J. Drug Targeting*, 2018, **26**, 884–894.

116 Y. Zhang, G. Jiang, W. Yu, D. Liu and B. Xu, *Mater. Sci. Eng., C*, 2018, **85**, 18–26.

117 L. Yang, Q. Liu, X. Wang, N. Gao, X. Li, H. Chen, L. Mei and X. Zeng, *Acta Pharm. Sin. B*, 2023, **13**, 344–358.

118 Y. Chen, B. Z. Chen, Q. L. Wang, X. Jin and X. D. Guo, *J. Controlled Release*, 2017, **265**, 14–21.

119 F. Zhao, D. Wu, D. Yao, R. Guo, W. Wang, A. Dong, D. Kong and J. Zhang, *Acta Biomater.*, 2017, **64**, 334–345.

120 T. Liu, G. Jiang, G. Song, Y. Sun, X. Zhang and Z. Zeng, *J. Pharm. Sci.*, 2021, **110**, 3004–3010.

121 B. Z. Chen, J. L. Liu, Q. Y. Li, Z. N. Wang, X. P. Zhang, C. B. Shen, Y. Cui and X. D. Guo, *ACS Appl. Bio Mater.*, 2019, **2**, 5616–5625.

122 Y. Zhao, T. Zhao, A. Zong and Y. Zhou, *Diabetes*, 2018, **67**, 2468–2475.

123 J. E. Gerich, *Endocr. Rev.*, 1998, **19**, 491–503.

124 A. J. Scheen, *Diabetes Metab.*, 2005, **31**, 5S27-25S34.

125 L. He, *Trends Pharmacol. Sci.*, 2020, **41**, 868–881.

126 G. M. Keating, *Drugs*, 2005, **65**, 1681–1692.

127 T. Minamii, M. Nogami and W. Ogawa, *J. Diabetes Invest.*, 2018, **9**, 701–703.

128 T. Adak, A. Samadi, A. Z. Ünal and S. Sabuncuoğlu, *Regul. Toxicol. Pharmacol.*, 2018, **92**, 324–332.

129 T. E. LaMoia and G. I. Shulman, *Endocr. Rev.*, 2021, **42**, 77–96.

130 A. Caturano, R. Galiero and P. C. Pafundi, *J. Am. Med. Assoc.*, 2019, **322**, 1312–1312.

131 Z. Lv and Y. Guo, *Front. Endocrinol.*, 2020, **11**, 191–201.

132 M. Fayfman, D. L. Mize, D. J. Rubin, I. Anzola, M. A. Urrutia, C. Ramos, F. J. Pasquel, J. Sonya Haw, P. Vellanki, H. Wang, K. E. Joyce, A. Karunakaran,

B. S. Albury, R. Weaver, L. Viswanathan, S. Jaggi, R. J. Galindo and G. E. Umpierrez, *Diabetes*, 2018, **67**, 1078–1085.

133 B. Cirincione and D. E. Mager, *Br. J. Clin. Pharmacol.*, 2017, **83**, 517–526.

134 M. B. Davidson, G. Bate and P. Kirkpatrick, *Nat. Rev. Drug Discovery*, 2005, **4**, 713–714.

135 P. Home, *Diabetes Res. Clin. Pract.*, 2021, **175**, 108816.

136 L. Moroder and H.-J. Musiol, *Angew. Chem., Int. Ed.*, 2017, **56**, 10656–10669.

137 Y. Chen, L. Huang, X. Qi and C. Chen, *Int. J. Mol. Sci.*, 2019, **20**, 5007–5023.

138 S. J. Pilla, J. R. Dotimas, N. M. Maruthur, J. M. Clark and H.-C. Yeh, *Diabetes Res. Clin. Pract.*, 2018, **139**, 221–229.

139 T. B. Stage, M.-M. H. Christensen, N. R. Jørgensen, H. Beck-Nielsen, K. Brøsen, J. Gram and M. Frost, *Bone*, 2018, **112**, 35–41.

140 D. Shen, H. Yu, L. Wang, X. Chen, J. Feng, Q. Zhang, W. Xiong, J. Pan, Y. Han and X. Liu, *J. Mater. Chem. B*, 2021, **9**, 6017–6028.

141 J. Yu, J. Wang, Y. Zhang, G. Chen, W. Mao, Y. Ye, A. R. Kahkoska, J. B. Buse, R. Langer and Z. Gu, *Nat. Biomed. Eng.*, 2020, **4**, 499–506.

142 Y. Zhang, M. Wu, W. Dai, Y. Li, X. Wang, D. Tan, Z. Yang, S. Liu, L. Xue and Y. Lei, *Nanoscale*, 2019, **11**, 6471–6479.

143 S. Chen, T. Miyazaki, M. Itoh, H. Matsumoto, Y. Moro-oka, M. Tanaka, Y. Miyahara, T. Suganami and A. Matsumoto, *ACS Appl. Polym. Mater.*, 2020, **2**, 2781–2790.

144 L. Yang, Y. Yang, H. Chen, L. Mei and X. Zeng, *Asian J. Pharm. Sci.*, 2022, **17**, 70–86.

145 V. Yesilyurt, M. J. Webber, E. A. Appel, C. Godwin, R. Langer and D. G. Anderson, *Adv. Mater.*, 2016, **28**, 86–91.

146 R. Ma, H. Yang, Z. Li, G. Liu, X. Sun, X. Liu, Y. An and L. Shi, *Biomacromolecules*, 2012, **13**, 3409–3417.

147 Z. Tong, J. Zhou, J. Zhong, Q. Tang, Z. Lei, H. Luo, P. Ma and X. Liu, *ACS Appl. Mater. Interfaces*, 2018, **10**, 20014–20024.

148 Y. Wang, S. Cheng, W. Hu, X. Lin, C. Cao, S. Zou, Z. Tong, G. Jiang and X. Kong, *Front. Mater. Sci.*, 2021, **15**, 98–112.

149 X.-X. Yang, P. Feng, J. Cao, W. Liu and Y. Tang, *ACS Appl. Mater. Interfaces*, 2020, **12**, 13613–13621.

150 Y. Lin, W. Hu, X. Bai, Y. Ju, C. Cao, S. Zou, Z. Tong, C. Cen, G. Jiang and X. Kong, *ACS Appl. Bio Mater.*, 2020, **3**, 6376–6383.

151 S. Gholami, I. Zarkesh, M.-H. Ghanian, E. Hajizadeh-Saffar, F. Hassan-Aghaei, M.-M. Mohebi and H. Baharvand, *Chem. Eng. J.*, 2021, **421**, 127823.

152 S. Chen, H. Matsumoto, Y. Moro-oka, M. Tanaka, Y. Miyahara, T. Suganami and A. Matsumoto, *Adv. Funct. Mater.*, 2019, **29**, 1807369.

153 J. Lv, G. Wu, Y. Liu, C. Li, F. Huang, Y. Zhang, J. Liu, Y. An, R. Ma and L. Shi, *Sci. China: Chem.*, 2019, **62**, 637–648.